NASA Technical Paper 1148

Analytical Study of Ride Smoothing Benefits of Control System Configurations Optimized for Pilot Handling Qualities

Bruce G. Powers

FEBRUARY 1978

NASA

NASA Technical Paper 1148

Analytical Study of Ride Smoothing Benefits of Control System Configurations Optimized for Pilot Handling Qualities

Bruce G. Powers

Dryden Flight Research Center
Edwards, California

National Aeronautics
and Space Administration

**Scientific and Technical
Information Office**

1978

ANALYTICAL STUDY OF RIDE SMOOTHING BENEFITS OF CONTROL SYSTEM CONFIGURATIONS OPTIMIZED FOR PILOT HANDLING QUALITIES

Bruce G. Powers
Dryden Flight Research Center

SUMMARY

An analytical study was conducted to evaluate the relative improvements in ride qualities that resulted from utilizing several control law configurations that were optimized for pilot handling qualities only. The airplane configuration used was an executive jet transport in the approach configuration. The control law configurations included the basic system, a rate feedback system, three command augmentation systems (rate command, attitude command, and rate command/attitude hold), and a control wheel steering system. Both the longitudinal and lateral-directional axes were evaluated. A representative example of each control law configuration was optimized for pilot handling qualities on a fixed-base simulator. The root mean square airplane responses to turbulence were calculated, and predictions of ride quality ratings were computed by using three models available in the literature.

In the longitudinal mode, the command augmentation systems reduced airplane normal acceleration response and flightpath angle disturbances due to turbulence compared with the basic and the rate feedback configurations. This was primarily due to the reduction of the phugoid motion. Similar reductions of the phugoid motion were also seen as a result of the pilot maintaining altitude. The calculated ride quality ratings showed only small improvements due to these response reductions.

In the lateral-directional axes, significant reductions in airplane roll rate, yaw rate, and lateral acceleration responses to turbulence were obtained with a rate feedback system. The command augmentation systems did not provide any significant benefit beyond that of the rate feedback system in reducing these responses; however, they did provide a significant reduction in bank angle and heading angle disturbances, which are of interest from a piloting standpoint. As a result, the lateral-directional command augmentation systems might be incorporated to improve the piloting task in turbulence, but they do not appear to provide a significant enough improvement when compared to the rate feedback system to warrant incorporation only to improve ride qualities.

There was a considerable difference in the effects of lateral-directional motion on the calculated ride quality ratings. For two of the ride quality rating models, lateral-directional motion had a negligible effect on the predicted ratings. For the other model, these motions made a major contribution to the calculated ride quality ratings.

INTRODUCTION

Precise maneuvering and flightpath control are required during landing approach, especially in the presence of turbulence. At the same time, smooth ride characteristics are desirable from both the pilot's and the passenger's standpoint. Most of the studies for improving ride qualities (refs. 1 to 4, for instance) have been directed toward gust alleviation systems which are separate from the pilot's control system. However, it has been shown that command augmentation systems designed to improve pilot handling qualities alone also improve ride qualities (ref. 5). Those limited results suggested that a systematic study was needed to quantify the improvements in ride qualities that could be expected from various handling-qualities-oriented control system concepts.

Therefore, an analytical study was conducted to evaluate the relative improvements in ride qualities due to several control law configurations. A model representing the JetStar airplane in the approach configuration was used for this study. The JetStar is a small, executive jet transport with a wing loading of 2870 N/m^2. The control law configurations, which were evaluated for both the longitudinal and the lateral-directional modes, included the basic airplane, a rate feedback system, three command augmentation systems (rate command, attitude command, and rate command/attitude hold), and a control wheel steering system. These configurations were optimized for pilot handling qualities on a fixed-base simulator to provide a representative example of each control law configuration for a comparison of the improvements in the ride qualities. The control laws evaluated in this study used only the conventional control surfaces—aileron, elevator, and rudder. An evaluation of control laws that incorporate direct lift and side force control surfaces for this airplane can be found in reference 6. The improvements in ride qualities were calculated in terms of airplane response to turbulence and also in terms of predicted ride quality ratings using the models in references 7 to 9.

SYMBOLS

a_n	vertical acceleration, g
a_x	longitudinal acceleration, g
a_y	lateral acceleration, g
b	wingspan, m

D	drag force divided by mass, m/sec^2
g	acceleration of gravity, m/sec^2
I_X	moment of inertia about longitudinal axis, $kg\text{-}m^2$
I_{XZ}	cross-product of inertia about longitudinal and normal axes, $kg\text{-}m^2$
I_Z	moment of inertia about normal axis, $kg\text{-}m^2$
K_i, S_i, $\dot{\bar{S}}_i$, $\bar{S}_{max}$, S_{Ti}	ride quality model parameters (ref. 9)
L	rolling moment divided by moment of inertia about longitudinal axis, $per\ sec^2$
$\bar{L}$	lift force divided by mass and velocity, rad/sec
L_w, L_v	vertical and horizontal turbulence scale length, m
M	pitching moment divided by moment of inertia about lateral axis, $per\ sec^2$
N	yawing moment divided by moment of inertia about normal axis, $per\ sec^2$
n_{z_α}	normal force due to angle of attack, g/rad
p	roll rate, deg/sec
p_g	roll rate due to turbulence, deg/sec
q	pitch rate, deg/sec
r	yaw rate, deg/sec
s	Laplace operator, per sec
V	velocity, m/sec
Y	side force divided by mass and velocity, per sec

α	angle of attack, deg
α_g	angle of attack due to turbulence, deg
β	angle of sideslip, deg
β_g	angle of sideslip due to turbulence, deg
γ	flightpath angle, $\theta - \alpha$, deg
Δ	increment
δ_a	aileron position, deg
δ_c	column position, cm
δ_e	elevator position, deg
δ_p	pedal position, cm
δ_r	rudder position, deg
δ_t	pilot trim input, deg
δ_w	wheel position, deg
$\delta_{w'}$	control wheel steering parameter, deg
ζ_d	Dutch-roll mode damping ratio
θ	pitch angle, deg
σ_w, σ_v	vertical and horizontal turbulence intensity, m/sec
$\Phi( )$	power spectral density of ( )
φ	bank angle, deg
φ_c	bank angle command, deg
ψ	heading, deg
ψ_c	heading command, deg

ω_d Dutch-roll mode natural frequency, rad/sec

Subscripts:

p, q, r, V, α, β, δ_a, δ_e, δ_r partial derivatives with respect to subscripted variable

0 nominal trim condition

A dot over a quantity denotes the time derivative of that quantity.

MATHEMATICAL DESCRIPTIONS OF AIRPLANE AND TURBULENCE

A six-degree-of-freedom, rigid-body model of the JetStar airplane (fig. 1) with constant, linear aerodynamic coefficients was used for this study. The analytical portion of the study used the following longitudinal linear equations:

$$\begin{bmatrix} \dot{\alpha} \\ \dot{q} \\ \dot{\theta} \\ \dot{V} \\ a_n \\ a_x \end{bmatrix} = \begin{bmatrix} -\bar{L}_\alpha & 1-\bar{L}_q & 0 & -\bar{L}_V \\ M_\alpha & M_q & 0 & M_V \\ 0 & 1 & 0 & 0 \\ -D_\alpha & 0 & -g & -D_V \\ \frac{V_0}{g}\bar{L}_\alpha & \frac{V_0}{g}\bar{L}_q & 0 & \frac{V_0}{g}\bar{L}_V \\ \frac{D_\alpha}{g} & 0 & 0 & \frac{D_V}{g} \end{bmatrix} \begin{bmatrix} \alpha \\ q \\ \theta \\ V \end{bmatrix} + \begin{bmatrix} -\bar{L}_{\delta_e} & -\bar{L}_\alpha \\ M_{\delta_e} & M_\alpha \\ 0 & 0 \\ 0 & -D_\alpha \\ \frac{V_0}{g}\bar{L}_{\delta_r} & \frac{V_0}{g}\bar{L}_\alpha \\ 0 & 0 \end{bmatrix} \begin{bmatrix} \delta_e \\ \alpha_g \end{bmatrix}$$

and the following lateral-directional equations:

$$\begin{bmatrix} 1 & \frac{-I_{XZ}}{I_X} & 0 & 0 & 0 \\ \frac{-I_{XZ}}{I_Z} & 1 & 0 & 0 & 0 \\ 0 & 0 & 1 & 0 & 0 \\ 0 & 0 & 0 & 1 & 0 \\ 0 & 0 & 0 & 0 & 1 \end{bmatrix} \begin{bmatrix} \dot{p} \\ \dot{r} \\ \dot{\beta} \\ \dot{\varphi} \\ \dot{a}_y \end{bmatrix} = \begin{bmatrix} L_p & L_r & L_\beta & 0 \\ N_p & N_r & N_\beta & 0 \\ \alpha_0 & -1 & Y_\beta & \frac{g}{V_0} \\ 1 & \theta_0 & 0 & 0 \\ 0 & 0 & \frac{V_0}{g}Y_\beta & 0 \end{bmatrix} \begin{bmatrix} p \\ r \\ \beta \\ \varphi \end{bmatrix} + \begin{bmatrix} L_{\delta_a} & L_{\delta_r} & L_\beta & L_p \\ N_{\delta_a} & N_{\delta_r} & N_\beta & N_p \\ Y_{\delta_a} & Y_{\delta_r} & Y_\beta & 0 \\ 0 & 0 & 0 & 0 \\ \frac{V_0}{g}Y_{\delta_a} & \frac{V_0}{g}Y_{\delta_r} & \frac{V_0}{g}Y_\beta & 0 \end{bmatrix} \begin{bmatrix} \delta_a \\ \delta_r \\ \beta_g \\ p_g \end{bmatrix}$$

Aerodynamic coefficients for the JetStar airplane were obtained from flight for the approach configuration at 140 knots airspeed. The numerical values for this condition, with angles in degrees and velocities in meters per second, are as follows.

For the longitudinal modes,

$$\begin{bmatrix} \dot{\alpha} \\ \dot{q} \\ \dot{\theta} \\ \dot{V} \end{bmatrix} = \begin{bmatrix} 0.863 & 1.000 & 0 & -0.065 \\ -1.976 & -0.918 & 0 & 0 \\ 0 & 1.000 & 0 & 0 \\ 0.077 & 0 & -0.172 & -0.038 \end{bmatrix} \begin{bmatrix} \alpha \\ q \\ \theta \\ V \end{bmatrix} + \begin{bmatrix} -0.075 & -0.863 \\ -2.579 & -1.976 \\ 0 & 0 \\ 0 & -0.077 \end{bmatrix} \begin{bmatrix} \delta_e \\ \alpha_g \end{bmatrix}$$

For the lateral-directional modes,

$$\begin{bmatrix} 1.000 & -0.088 & 0 & 0 \\ -0.028 & 1.000 & 0 & 0 \\ 0 & 0 & 1.000 & 0 \\ 0 & 0 & 0 & 1.000 \end{bmatrix} \begin{bmatrix} \dot{p} \\ \dot{r} \\ \dot{\beta} \\ \dot{\varphi} \end{bmatrix} =$$

$$\begin{bmatrix} -0.974 & 0.385 & -4.090 & 0 \\ -0.163 & -0.163 & 0.884 & 0 \\ 0.192 & -1.000 & -0.122 & 0.136 \\ 1.000 & 0.192 & 0 & 0 \end{bmatrix} \begin{bmatrix} p \\ r \\ \beta \\ \varphi \end{bmatrix} + \begin{bmatrix} 1.378 & 0.697 & -4.090 & -0.974 \\ 0.089 & -0.606 & 0.884 & -0.163 \\ -0.006 & 0.047 & -0.122 & 0 \\ 0 & 0 & 0 & 0 \end{bmatrix} \begin{bmatrix} \delta_a \\ \delta_r \\ \beta_g \\ p_g \end{bmatrix}$$

Three components of turbulence were used: α_g, β_g, and p_g. For ease in programing the simulator, α_g and β_g were mechanized as first-order approximations of the Dryden turbulence model. These first-order approximations were also used for the analytical calculations. The power spectral densities resulting from these equations are compared to the Dryden model in figure 2, and the transfer functions of the turbulence components to the three independent white noise sources are shown below.

Parameter	Transfer function
α_g	$\dfrac{\frac{-57.3\sigma_w}{V_0}\sqrt{\frac{L_w}{\pi V_0}}}{1+\frac{L_w}{\sqrt{3}V_0}s}$
β_g	$\dfrac{\frac{-57.3\sigma_v}{V_0}\sqrt{\frac{L_v}{\pi V_0}}}{1+\frac{L_v}{\sqrt{3}V_0}s}$
p_g	$\dfrac{57.3\sigma_w\sqrt{\frac{0.8\left(\frac{\pi L_w}{4b}\right)^{1/3}}{L_w V_0}}}{1+\frac{4b}{\pi V_0}s}$

The values of the constants for the JetStar airplane used in this study are as follows: $L_w = L_v = 533$ meters; $V_0 = 72.5$ meters per second; $b = 16.6$ meters; and $\sigma_w = \sigma_v$, in meters per second.

HANDLING QUALITIES DESIGN CRITERIA

Closed Loop Criteria

The criteria in reference 10 (for category C, level 1 aircraft) were used to establish the closed loop characteristics for the various control law configurations. In the longitudinal modes, reference 10 required a short-period frequency ranging from 1.00 radian per second to 4.77 radians per second (for n_{z_a} equal to 6.3 g's per radian), a short-period damping ratio from 0.35 to 1.30, and a phugoid damping ratio greater than 0.04. The desired short-period characteristics were selected within these ranges, and this resulted in short-period design goals of 2.00 radians per second for the natural frequency and of 0.65 for the damping ratio. Any additional modes introduced by the augmentation system were arbitrarily required to have a damping ratio of greater than 0.70. No restriction was placed on frequency for the additional modes, although an effort was made to separate the frequencies of these modes from the frequency of the short-period mode as much as possible. For the lateral-directional characteristics (ref. 10), the Dutch-roll mode requirements were ω_d greater than or equal to 0.4 radian per second and $\zeta_d\omega_d$ greater than or equal to 0.15. The design goals for this study were selected as ζ_d equal to 0.50 and ω_d greater than 1.0 radian per second. All other modes were required to be stable, and any additional augmentation system modes were required to have damping ratios greater than 0.70.

Response Criteria for Command Augmentation Systems

For the response of the commanded quantity due to pilot input in the command augmentation systems, the bandwidth (at the -3 dB point) was required to be greater than the desired natural frequency values for the short-period and Dutch-roll modes. This provided a longitudinal bandwidth of 2.0 radians per second and a lateral-directional bandwidth of 1.0 radian per second. In addition, the frequency response curves were required to be within an envelope of 1 decibel to -3 decibels for frequencies less than the desired natural frequencies and phase angles greater than -60° at 1 radian per second. An additional constraint, based on the requirement in reference 11 for attitude command systems, was added to the time response: that the commanded parameter reach 90 percent of its steady-state value in less than 2.0 seconds for a step input in pilot command.

Other Design Considerations

For the rate feedback systems, only angular rate feedbacks and pilot control to surface feedforwards were allowed. Compensators were limited to washout networks. The rate command system feedback parameters were limited to angular rates; various forms of feedforwards and compensators were allowed. For the attitude command and rate command/attitude hold systems, attitude feedbacks were allowed in addition to those items for the rate command systems. Based on previous

experience with the JetStar airplane, feedback gains were limited to 2.0° of surface deflection per degree of attitude and 2.0° of surface deflection per degree per second of angular rate.

DESCRIPTION OF CONTROL LAW CONFIGURATIONS

The control law configurations were developed analytically by using the previously described design criteria. The configurations were then refined on a fixed-base simulator to establish a representative example of each control law configuration with satisfactory handling qualities. The resulting control law configurations and their characteristics are shown in figures 3 to 13. Part (a) of each figure shows a block diagram of the system and the gains used; part (b) shows the frequency response of the controlled variable; and part (c) shows the time history of the response to a step command.

Longitudinal Control Law Configurations

Basic system.—A block diagram of the basic longitudinal control system is shown in figure 3(a). This system commanded elevator position proportional to column displacement and, as is apparent from the plots of frequency response in figure 3(b) and of the time response in figure 3(c), it approximated an angle of attack command system. For the short-period transient time response, this system also approximated a pitch rate command system, as shown in figure 3(c). Pitch rate decreased with time, however, so a pitch angle response proportional to column displacement was achieved for the steady-state response.

Rate feedback system.—The longitudinal rate feedback system is shown in figure 4. This system was essentially the same as the basic system. Only a slight amount of pitch rate feedback was required to increase the basic configuration's short-period damping ratio to the desired level in the design criteria.

Rate command system.—A block diagram of the pitch rate command system is shown in figure 5(a). A lag-lead-compensated pitch rate feedback combined with a proportional-plus-integral network was used to provide a pitch rate response that was proportional to column displacement over a wide frequency range (fig. 5(b)). Although not strictly within the constraints, the low frequency droop in the frequency response produced a slight reduction in pitch rate response with time, as shown in the plot of time response (fig. 5(c)). This was not considered to be important.

Attitude command system.—A block diagram of the attitude command system is shown in figure 6(a). Pitch attitude and pitch rate were fed back through a second-order compensator to a proportional-plus-integral network. This system provided an airplane pitch attitude response proportional to pilot input (fig. 6(c)).

Rate command/attitude hold system.—A block diagram of the rate command/attitude hold system is shown in figure 7(a). The pitch attitude and pitch rate feedback provided the attitude hold part of the system. The rate command part of the system was provided by a compensated pilot input, which included a lead-lag

network and a proportional-plus-integral network. The integral network in the feedforward provided a pitch rate response that was proportional to pilot input, as shown in figure 7(c). For no pilot input, the system maintained pitch attitude. This system was also used as the longitudinal portion of the control wheel steering system.

Lateral-Directional Control Law Configurations

Basic system.—The block diagram of the basic lateral-directional system is shown in figure 8(a). The most prominent characteristic of the system was very low Dutch-roll damping, as indicated by the amplification of the roll rate response near a frequency of 1.3 radians per second in figure 8(b). This system provided a highly oscillatory roll rate response that was approximately proportional to pilot input, as shown in figure 8(c).

Rate feedback system.—The rate feedback system block diagram is shown in figure 9(a). Washed-out yaw rate feedback to the rudder was used to improve the Dutch-roll damping, and roll rate feedback to the aileron was used to improve the roll damping. A wheel-to-rudder interconnect and roll rate feedback to the rudder were used to improve turn coordination. The frequency response near the Dutch-roll frequency (fig. 9(b)) was better than in the basic airplane, and the time response (fig. 9(c)) shows that roll rate response was proportional to pilot input.

Rate command system.—The roll rate command system is shown in figure 10(a). This system was essentially the same as the rate feedback system with the addition of a proportional-plus-integral compensator in the roll axis. Because of the higher effective gains, a low pass filter was added to the pilot input to reduce the peak aileron values for sharp pilot inputs. The frequency response at the low frequencies (fig. 10(b)) is improved by the integral compensations. The time response (fig. 10(c)) shows roll rate response to be proportional to pilot input.

Attitude command system.—The roll attitude command system is shown in figure 11(a). Roll rate and attitude were fed back to the ailerons, and roll and yaw rates were fed back to the rudder. No washout was required on yaw rate, since spiral stability was controlled through the roll axis. Pilot inputs were shaped to provide the frequency response shown in figure 11(b) and to limit the peak aileron values for sharp pilot inputs. Figure 11(c) shows the roll attitude time response to be proportional to the pilot input.

Rate command/attitude hold system.—The rate command/attitude hold system is shown in figure 12(a). The attitude hold part of the system was similar to the attitude command system with bank angle feedback to the rudder added to improve the steady-state turn coordination. The pilot input compensator consisted of a proportional-plus-integral network, which provided roll rate response proportional to pilot input (figs. 12(b) and 12(c)).

Control wheel steering.—The control wheel steering system (fig. 13) consisted of the rate command/attitude hold system with the addition of a heading hold when there was no pilot input and the bank angle was less than 7°. This system was designed within the requirements of reference 12 for control wheel steering systems.

A block diagram of the system is shown in figure 13(a). For wheel deflections greater than 6° or bank angles greater than 7°, the roll rate command/attitude hold system was engaged. For wheel deflections less than 6° and bank angles less than 7°, the heading hold system was engaged. A network of the track and hold type was used to establish the commanded heading. With this network, the pilot could maneuver (with bank angle greater than 7°) to a new heading, roll back to a bank angle less than 7°, and maintain the new heading upon releasing the control. A trim input was required to provide a vernier control of the commanded heading. A bandwidth of 0.3 radian per second was selected from the simulator evaluations. The frequency response of the heading hold mode is shown in figure 13(b). For a step heading command input to the trip system, the time to 90 percent of the commanded value was approximately 7 seconds, as shown in figure 13(c).

AIRPLANE RESPONSE TO TURBULENCE

After establishing a representative example of each control law configuration, the airplane's responses for a 0.3-meter-per-second rms turbulence input with no pilot input were calculated for each turbulence component (α_g, β_g, and p_g). Power spectral densities were calculated over the frequency range from 0.01 radian per second to 80 radians per second. The lateral-directional parameters included the effects of the β_g and p_g components of turbulence. The rms values of the responses for all of the control system configurations are summarized in table 1, and the power spectral densities of selected parameters are shown in figure 14.

TABLE 1.—RMS RESPONSES TO 0.3-METER-PER-SECOND TURBULENCE INPUT FOR VARIOUS CONTROL SYSTEM CONFIGURATIONS

	Basic	Rate feedback	Rate command	Attitude command	Rate command/ attitude hold	Control wheel steering
a_n, g	0.01336	0.01266	0.00958	0.00978	0.00972	0.00972
a_y, g	0.00396	0.00156	0.00123	0.00132	0.00137	0.00161
a_x, g	0.00367	0.00368	0.00362	0.00371	0.00364	0.00364
$\dot{p}$, deg/sec^2	1.0397	0.3977	0.3876	0.3643	0.3397	0.3506
$\dot{q}$, deg/sec^2	0.1535	0.1366	0.1131	0.1230	0.1064	0.1064
$\dot{r}$, deg/sec^2	0.3388	0.1157	0.0980	0.1047	0.1043	0.1108
p, deg/sec	0.7350	0.2137	0.1750	0.1524	0.1244	0.1480
q, deg/sec	0.1055	0.0895	0.0464	0.0417	0.0362	0.0362
r, deg/sec	0.3064	0.1384	0.0750	0.0829	0.0820	0.0914
δ_a, deg	0	0.1707	0.2450	0.2615	0.2824	0.2808
δ_e, deg	0	0.0179	0.0836	0.1150	0.0881	0.0881
δ_r, deg	0	0.1269	0.1348	0.1227	0.1228	0.1386
φ, deg	1.4390	0.8273	0.1832	0.1463	0.1162	0.2356
θ, deg	0.5021	0.4811	0.0853	0.0298	0.0804	0.0804
ψ, deg	13.0900	7.7240	0.2148	0.2605	0.2499	0.1493
α, deg	0.2116	0.2043	0.1706	0.1767	0.1686	0.1686
β, deg	0.3702	0.2465	0.2236	0.2200	0.2167	0.2210
γ, deg	0.4414	0.4301	0.1667	0.1660	0.1724	0.1724

In the longitudinal mode (table 1), the rate feedback configuration caused little change in the rms response to turbulence of the parameters most significant to ride qualities (a_n, $\dot{q}$, and q), whereas the command augmentation configurations caused a reduction. The rate feedback configuration affected primarily the short-period motion, whereas the command augmentation configurations significantly improved the phugoid damping in addition to the short-period damping. The command augmentation systems reduced the pitch rate motion about 60 percent and the normal acceleration about 28 percent compared to the motion of the basic airplane system. In the lateral-directional mode, the most significant reduction in motion is the change from the basic airplane to the rate feedback configuration, which is the result of the increased Dutch-roll damping. Roll rate motion was reduced 71 percent, yaw rate motion 55 percent, and lateral acceleration 61 percent. An additional reduction in motion on the order of 10 percent to 20 percent for these parameters can be seen for the command augmentation configurations.

From a piloting standpoint the most significant variables are probably the airplane's attitude (bank angle and pitch angle) and the airplane's direction of flight (flightpath angle and heading angle). The improvements of the command augmentation configurations on the rate feedback and basic airplane configurations are obvious in both the longitudinal and lateral-directional modes. The flightpath angle deviations for the command augmentation configurations are about 40 percent and the heading deviations are about 3 percent of the rate feedback configuration deviations; bank and pitch angle deviations are 20 percent to 30 percent of the rate feedback configuration values. An examination of the power spectral densities of pitch angle (fig. 14(b)) and roll angle (fig. 14(e)) shows that the command augmentation configurations reduced the airplane attitude response to turbulence over the entire frequency range. The flightpath angle responses (fig. 14(a)) are reduced by the command augmentation systems at frequencies below the phugoid frequency (0.3 rad/sec) and above the short-period frequency (1.5 rad/sec). The increase in the response to turbulence at frequencies from 0.3 radian per second to 1.0 radian per second is due primarily to the modes introduced by the command augmentation configuration compensators. The heading angle response to turbulence for the command augmentation systems (fig. 14(d)) is reduced compared to the rate feedback system, especially at the lower frequencies.

COMPUTED RIDE QUALITY RATINGS

To gain some perspective about the significance of the aircraft motions from the passenger's viewpoint, ride quality ratings were computed using the ride quality rating models in references 7 to 9. (The rating models are described in the appendix.) The reference 7 model includes the effects of motion in six degrees of freedom, the three angular accelerations, and the three linear accelerations. Reference 7 also presents a model that contains a function of frequency; however, this function is a constant for frequencies from 0 hertz to 20 hertz except for an amplification of the motion in the 2- to 5-hertz region. Since the rigid-body JetStar model did not have significant motion above 2 hertz for any of the control law configurations, this frequency-dependent model was not used. The reference 8 model includes only the effects of lateral and normal acceleration. The reference 9 model includes the effects of the three angular rates and the three linear accelerations.

The ride quality ratings calculated for the various control law configurations by using these models are shown in figure 15 as a function of input turbulence. Also included for comparison with the reference 8 and 9 models are the results for a ride smoothing system described in reference 6 that incorporates direct lift and side force surfaces. The ratings for the reference 7 and 8 models show a linear relationship with turbulence intensity. The ratings range from comfortable with no turbulence to acceptable with severe turbulence. For the severe turbulence level, the rate feedback configuration improves the ride rating approximately 0.2 above the basic airplane and the command augmentation systems improve the rating about 0.2 above that. The reference 6 ride smoothing system provides an additional increment of about 0.2 above the command augmentation systems.

The ride quality ratings using the reference 9 model (fig. 15(c)) show a nonlinear trend with turbulence intensity. These ratings indicate that the basic airplane would range from very comfortable for no turbulence to very uncomfortable for heavy and severe turbulence. The rate feedback system improves the ratings for heavy and severe turbulence to uncomfortable, and all of the command augmentation systems improve the rating for severe turbulence to acceptable. With this ride quality rating model, the reference 6 ride smoothing system has about the same effect as the rate feedback configuration.

The three ride rating models are in reasonable agreement with one another for the command augmentation configurations, the maximum spread between the ratings being approximately 0.75. Since the differences for the basic airplane are much larger, it is of interest to examine the influence of the individual airplane motions that make up the ride quality ratings. The reference 7 model consists of a summation of the effects of the individual motions. The relative importance of each type of motion to the ride quality rating is shown in figure 16(a). The two components of the reference 8 model are summed in a similar manner and are shown in figure 16(b). Both of these models indicate that the ride quality ratings are dominated by the normal acceleration response for all control law configurations. The reference 6 ride smoothing system reduced the relative effect of the normal acceleration response to about 60 percent of that of the basic configuration. The command augmentation systems reduced the relative effect to about 75 percent of the basic configuration, thus producing about 60 percent of the improvement of the ride smoothing system.

For the reference 9 model, the rating is based on the maximum effective motion plus an additional amount for the other motions. The relative effect of each of the motions is shown in figure 16(c) for turbulence intensities of 0.3 meter per second and 2.1 meters per second. With this model, the ride ratings of the basic airplane are strongly related to roll rate and yaw rate. With the command augmentation control law configurations, the effect of lateral-directional motion is at about the same level as the effect of normal acceleration, especially at the higher turbulence intensities. Thus, the primary difference between this model and the previous two is the importance of lateral-directional motion. When lateral-directional motion is reduced (as it is with the command augmentation systems), the results of all three models are similar. The disagreement between the models when lateral-directional motion is great is of concern for the control system designer, however. The reference 7 and 8 models would indicate that very little effort should be spent in reducing the lateral-directional motion, whereas the reference 9 model would indicate that this type of motion should receive a major level of effort. As an

example, the reference 6 ride smoothing system (figs. 16(b) and 16(c)) was designed by using the reference 8 ride quality model. As would be expected, good results were obtained using this model, but the improvements were judged only fair by the reference 9 model. The use of the reference 9 model would probably result in a more conservative design.

Another area of concern in using these ride quality rating models is the effect of the low frequency content of the motions. The results shown in the previous figures are for an unpiloted vehicle. Usually a pilot is maintaining the flight condition with a feedback control, which tends to eliminate the low frequency response to turbulence. As an example, the normal acceleration power spectral density for loose altitude control (3.3-second time constant) is shown in figure 17 for the basic configuration and the rate command/attitude hold configuration. The response around the phugoid frequency (0.16 rad/sec) is greatly reduced. The rms responses for the two control systems are more nearly the same with the pilot holding altitude, although the frequency content near the short period is different.

The three ride quality rating models used did not contain any functions of frequency. Although reference 7 presented a frequency-dependent model, it contained no variations with frequencies below 2 hertz. Other frequency-dependent ride quality criteria are presented in reference 13, and the normal acceleration criterion is reproduced in figure 18 with the nonpiloted responses for the various control law configurations. It is apparent that the control systems are only effective below approximately 0.5 hertz and that some of the reductions in the short-period motions at approximately 0.25 hertz may be significant in terms of this criterion. There is no indication from this criterion that motion around the phugoid frequency (0.025 Hz) is significant. Unfortunately, this criterion has not been completely validated. This criterion does raise questions, however, about the significance of the reductions in motion that can be achieved by control systems or by pilot control inputs in the longitudinal mode below 0.1 hertz.

CONCLUDING REMARKS

Airplane response to turbulence was calculated for several control law configurations that were optimized for pilot handling qualities only. The control law configurations included the basic system, a rate feedback system, three command augmentation systems (rate command, attitude command, and rate command/attitude hold), and a control wheel steering system for both the longitudinal and lateral-directional axes.

In the longitudinal mode, the command augmentation systems showed a reduction in airplane response to turbulence over the basic and the rate feedback configurations for the motion parameters of interest to both the passenger and the pilot. With the command augmentation systems, normal accelerations were reduced about 28 percent and flightpath angle disturbances were reduced about 60 percent compared with the basic airplane. This was due primarily to a reduction in phugoid motion and to a lesser extent to a reduction in short-period motion. A significant reduction in phugoid motion was also seen as the result of pilot inputs made to maintain level flight. The calculated ride quality ratings using three models available in the

literature showed only small improvements due to these response reductions and were in good agreement with one another for the longitudinal motions. The command augmentation systems provided an incremental improvement in ride quality of about 60 percent over that provided by a ride smoothing system described in a previous study that used a direct lift flap.

In the lateral-directional axes, significant reductions in airplane response to turbulence were obtained with a rate feedback system. The system provided reductions in roll rate motion of 71 percent, in yaw rate of 55 percent, and in lateral acceleration of 61 percent. With the command augmentation systems, additional reductions of 10 percent to 20 percent were achieved for these parameters.

Although the command augmentation systems did not significantly reduce the response due to turbulence of the parameters of interest for ride qualities when compared to the rate feedback system, they did provide a significant reduction of the responses of interest from a piloting standpoint compared with the rate feedback system. As a result, the command augmentation systems might be incorporated to improve the piloting task in turbulence, but they do not appear to provide a significant enough improvement when compared to the rate feedback system to warrant incorporation only to improve ride qualities.

There was a considerable difference in the effect of the lateral-directional motion on the calculated ride quality ratings. For two of the ride quality rating models, the lateral-directional motion had a negligible effect on the predicted ratings. For the other model, these motions made a major contribution to the calculated ride quality ratings.

Dryden Flight Research Center
National Aeronautics and Space Administration
Edwards, Calif., September 8, 1976

APPENDIX—RIDE QUALITY RATING MODELS

The ride quality rating models in references 7 to 9 are shown here for the convenience of the reader. These models use the following rating scale:

Rating	Ride description
1	Very comfortable
2	Comfortable
3	Acceptable
4	Uncomfortable
5	Very uncomfortable

Reference 7 Model

This model uses the rms values of linear and angular accelerations to create the ride quality rating.

$$\text{Rating} = 1.8 + 11.5\bar{a}_n + 5.0\bar{a}_y + 1.0\bar{a}_x + 0.25\dot{\bar{q}} + 0.4\dot{\bar{p}} + 1.9\dot{\bar{r}}$$

where $\bar{a}_n$, $\bar{a}_y$, and $\bar{a}_x$ are the rms linear accelerations in g's along the vertical, transverse, and longitudinal axes and $\dot{\bar{q}}$, $\dot{\bar{p}}$, and $\dot{\bar{r}}$ are the rms angular accelerations in rad/sec^2 about the pitch, roll, and yaw axes.

Reference 8 Model

This model uses transverse and vertical acceleration. For cases where the vertical accelerations are greater than 1.6 times the transverse accelerations, as for the JetStar airplane, the ratings are arrived at as follows:

$$\text{Rating} = 2.0 + 7.6\bar{a}_y + 11.9\bar{a}_n$$

where $\bar{a}_y$ and $\bar{a}_n$ are the rms transverse and vertical accelerations in g's.

Reference 9 Model

This model uses the rms values of the linear accelerations and the angular rates to form the ride quality rating, as follows:

$$\text{Rating} = 1 + \log_{10}\bar{S}_{max} + 0.000176(\log_{10}\bar{S}_{max})^4\left[(\log_{10}\bar{S}_i)^4 - (\log_{10}\bar{S}_{max})^4\right]$$

where

$\bar{S}_i = \left(\frac{S_i}{S_{Ti}}\right)^{K_i}$

$\bar{S}_{max}$ maximum value of the components, S_i

$\frac{S_i}{S_{Ti}}$ ratio of the rms value of the ith parameter to the threshold value; $\frac{S_i}{S_{Ti}} = 0$ for $S_i < S_{Ti}$

The values used for S_{Ti} and K_i are shown in the following table.

Motion variable	S_{Ti}	K_i
Pitch rate, rad/sec	0.000244	0.99
Roll rate, rad/sec	0.000166	0.65
Yaw rate, rad/sec	0.000763	1.94
Longitudinal acceleration, g . .	0.000767	1.10
Transverse acceleration, g . .	0.001220	1.14
Vertical acceleration, g . . .	0.002990	1.57

REFERENCES

1. Gordon, C. K.; and Dodson, R. D.: STOL Ride Control Feasibility Study. NASA CR-2276, 1973.

2. Lallman, Frederick J.: Gust Alleviation for a STOL Transport by Using Elevator, Spoilers, and Flaps. NASA TN D-7559, 1974.

3. Barnes, A. G.: C.S.A.S. Design for Good Handling in Turbulence. Flight in Turbulence, AGARD-CP-140, Nov. 1973, pp. 21-1—21-4.

4. Oehman, Waldo I.: Analytical Study of the Performance of a Gust Alleviation System for a STOL Airplane. NASA TN D-7201, 1973.

5. Loschke, Paul C.; Barber, Marvin R.; Enevoldson, Einar K.; and McMurtry, Thomas C.: Flight Evaluation of Advanced Control Systems and Displays on a General Aviation Airplane. NASA TN D-7703, 1974.

6. Lapins, Maris; and Jacobson, Ira D.: Application of Active Controls Technology to Aircraft Ride Smoothing Systems. NASA CR-145980, 1975.

7. Kuhlthau, A. R.; and Jacobson, Ira D.: Investigation of Traveler Acceptance Factors in Short-Haul Air Carrier Operations. Symposium on Vehicle Ride Quality, NASA TM X-2620, 1972, pp. 211-228.

8. Jacobson, I. D.; and Richards, L. G.: Ride Quality Evaluation. II—Modelling of Airline Passenger Comfort. Ergonomics, vol. 19, Jan. 1976, pp. 1-10.

9. Stone, Ralph W., Jr.: Ride Quality - An Exploratory Study and Criteria Development. NASA TM X-71922, 1974.

10. Flying Qualities of Piloted Airplanes. Military Specification MIL-F-8785B (ASG), Aug. 7, 1969.

11. V/STOL Handling-Qualities Criteria. I - Criteria and Discussion. AGARD Rept. No. 577, Dec. 1970.

12. Flight Control Systems—Design, Installation and Test of, Piloted Aircraft, General Specification for Military Specification MIL-F-9490C (USAF), Mar. 13, 1964.

13. Stone, Ralph W., Jr.: Ride-Quality Overview. Symposium on Vehicle Ride Quality, NASA TM X-2620, 1972, pp. 1-22.

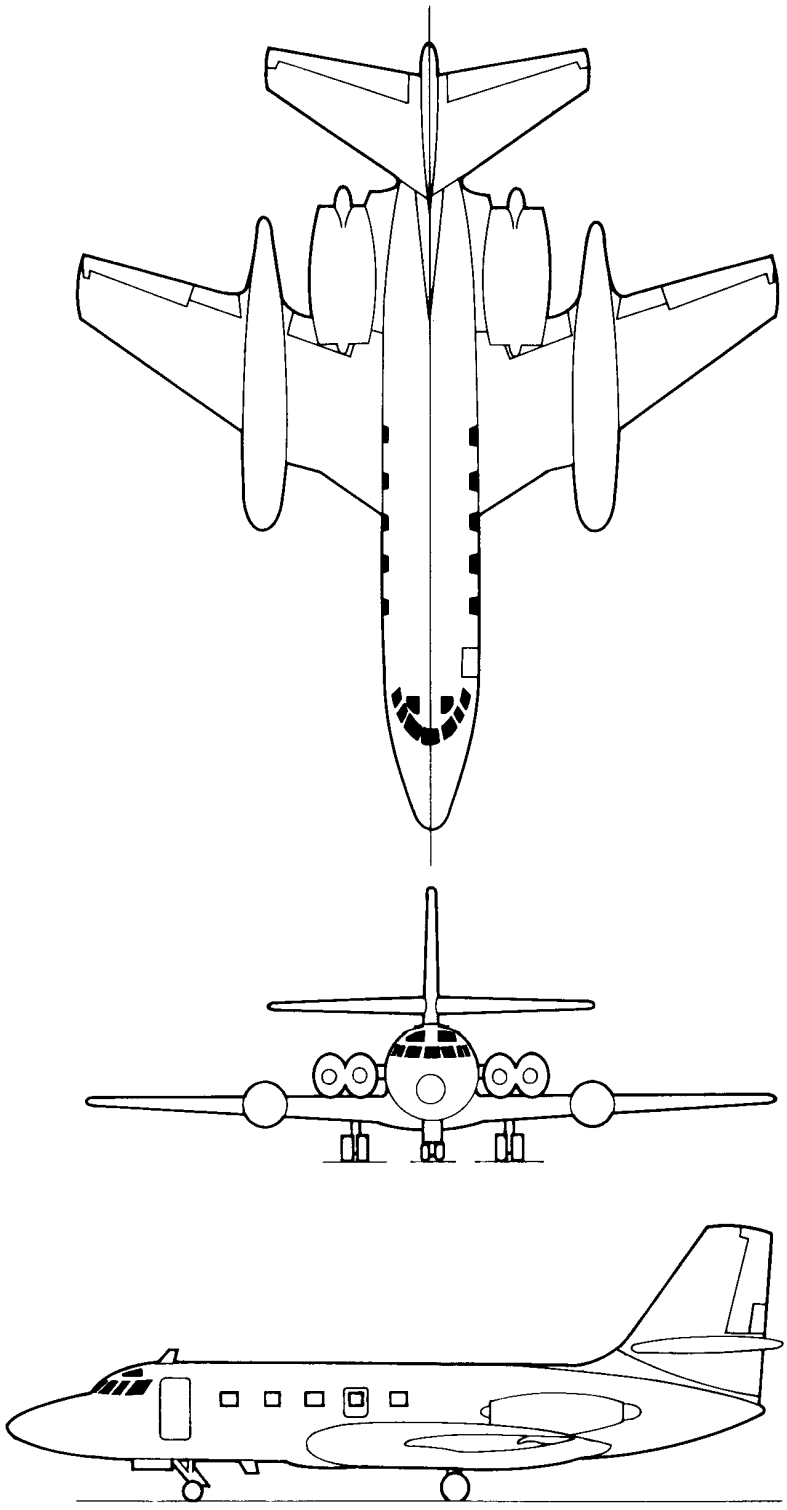

Figure 1. Three-view drawing of JetStar airplane. Airplane wingspan = 16.5 m; length = 18.44 m; height = 6.25 m.

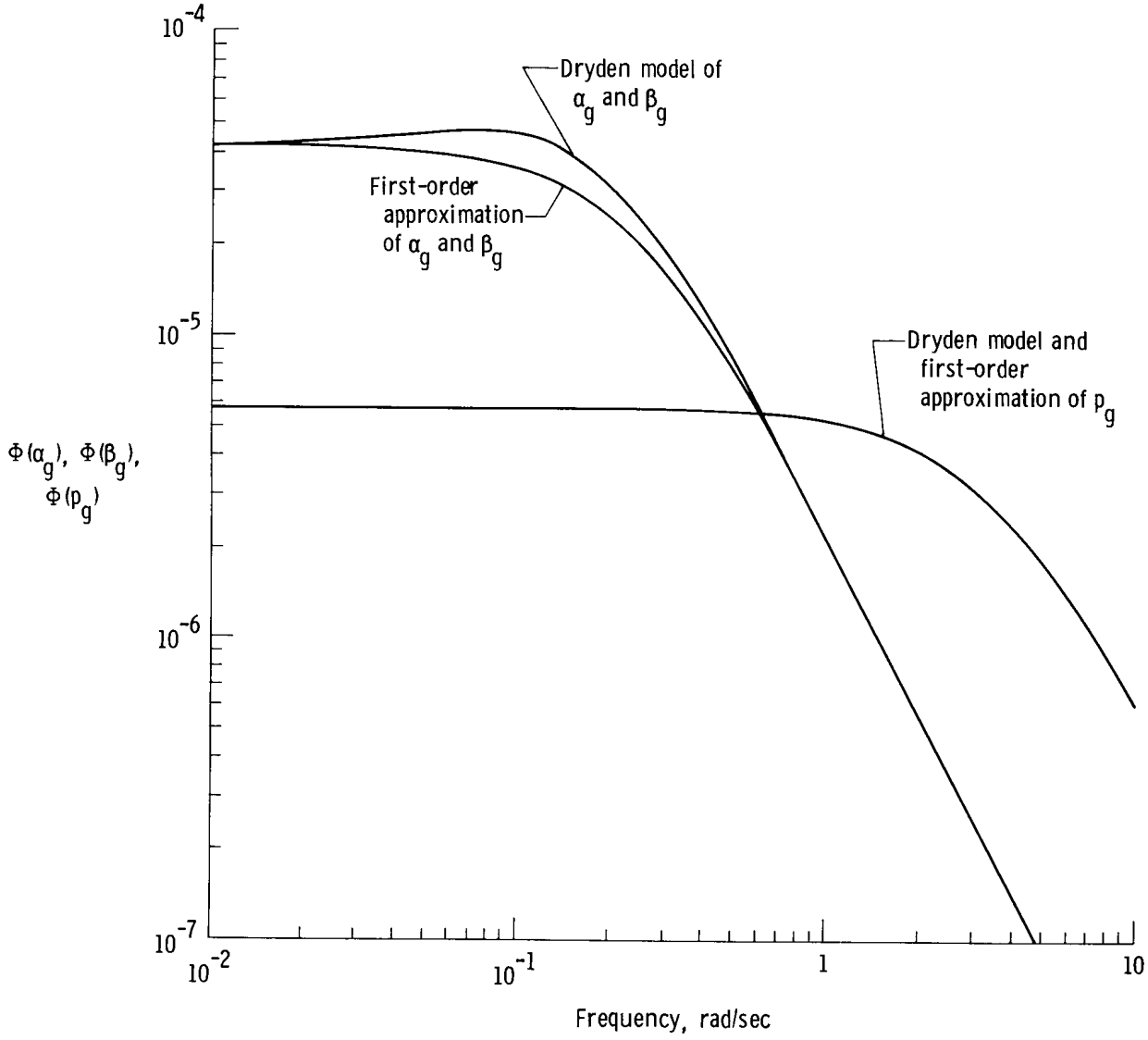

Figure 2. Comparison of first-order turbulence model used in this program with Dryden turbulence model.

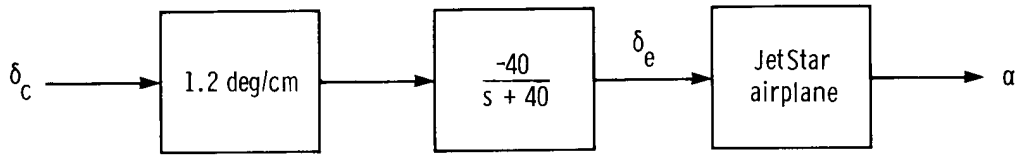

(a) Block diagram.

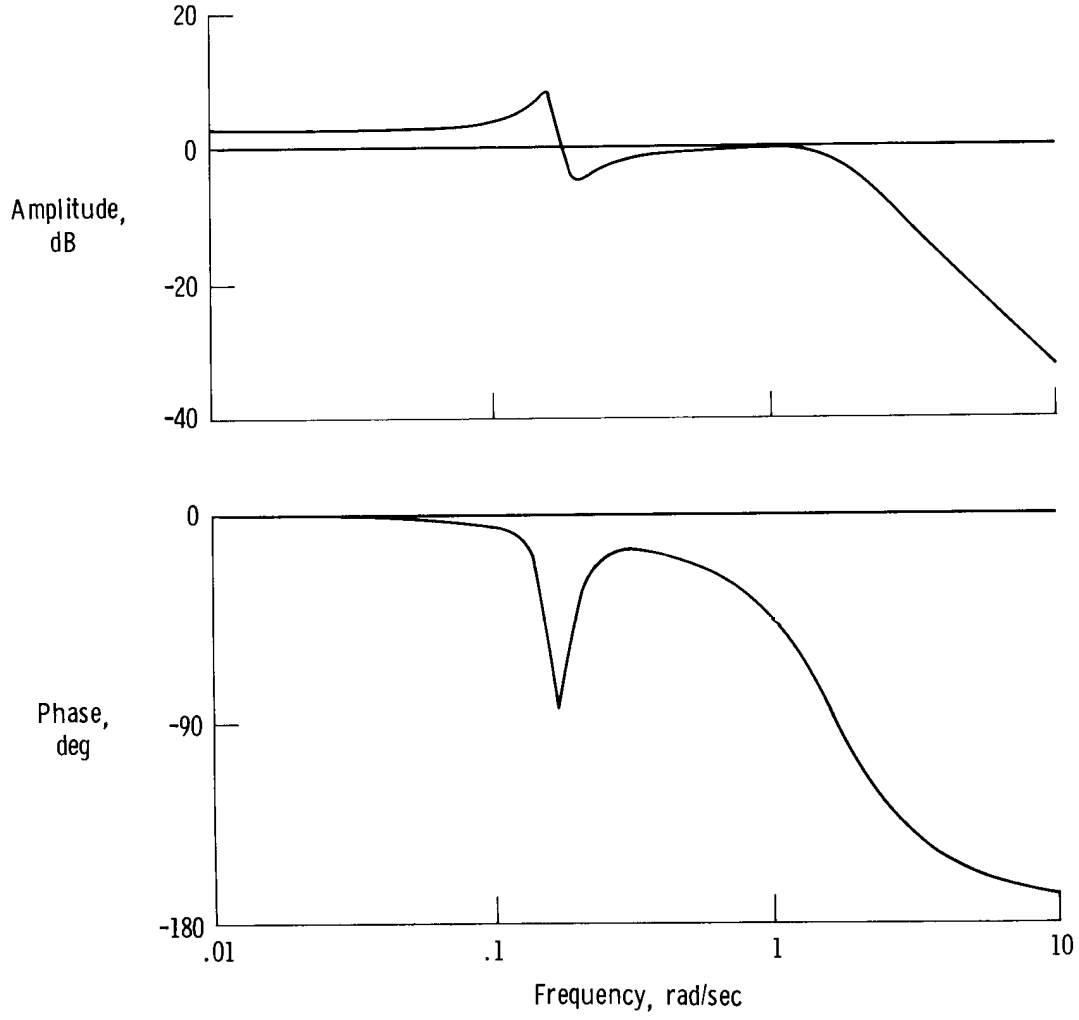

(b) Frequency response of α/δ_c.

Figure 3. Basic longitudinal control system.

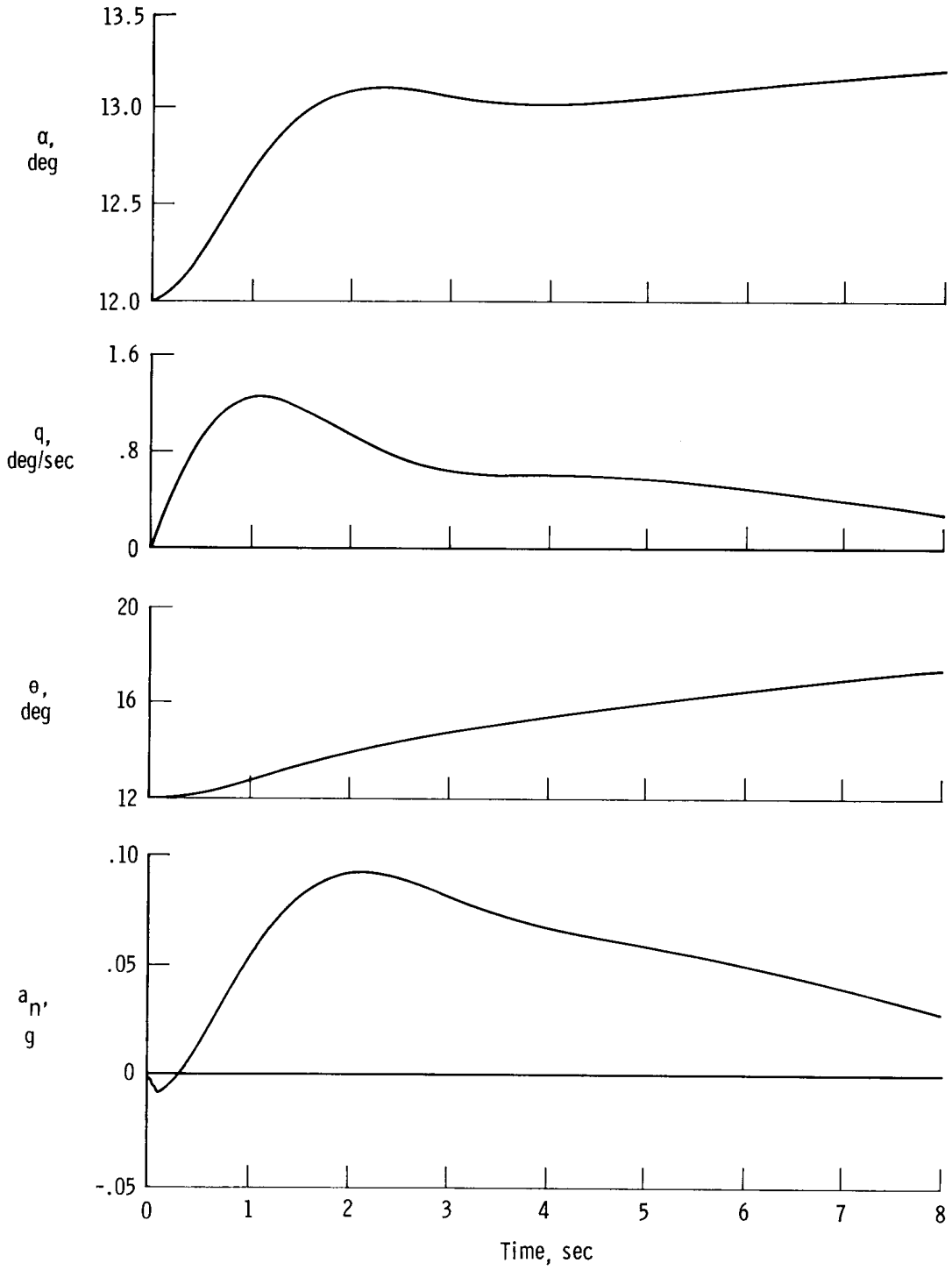

(c) Time response.

Figure 3. Concluded.

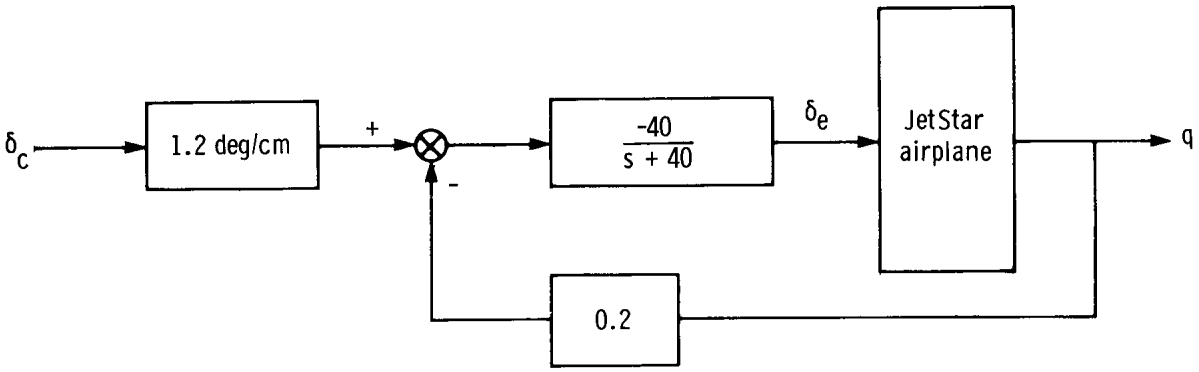

(a) Block diagram.

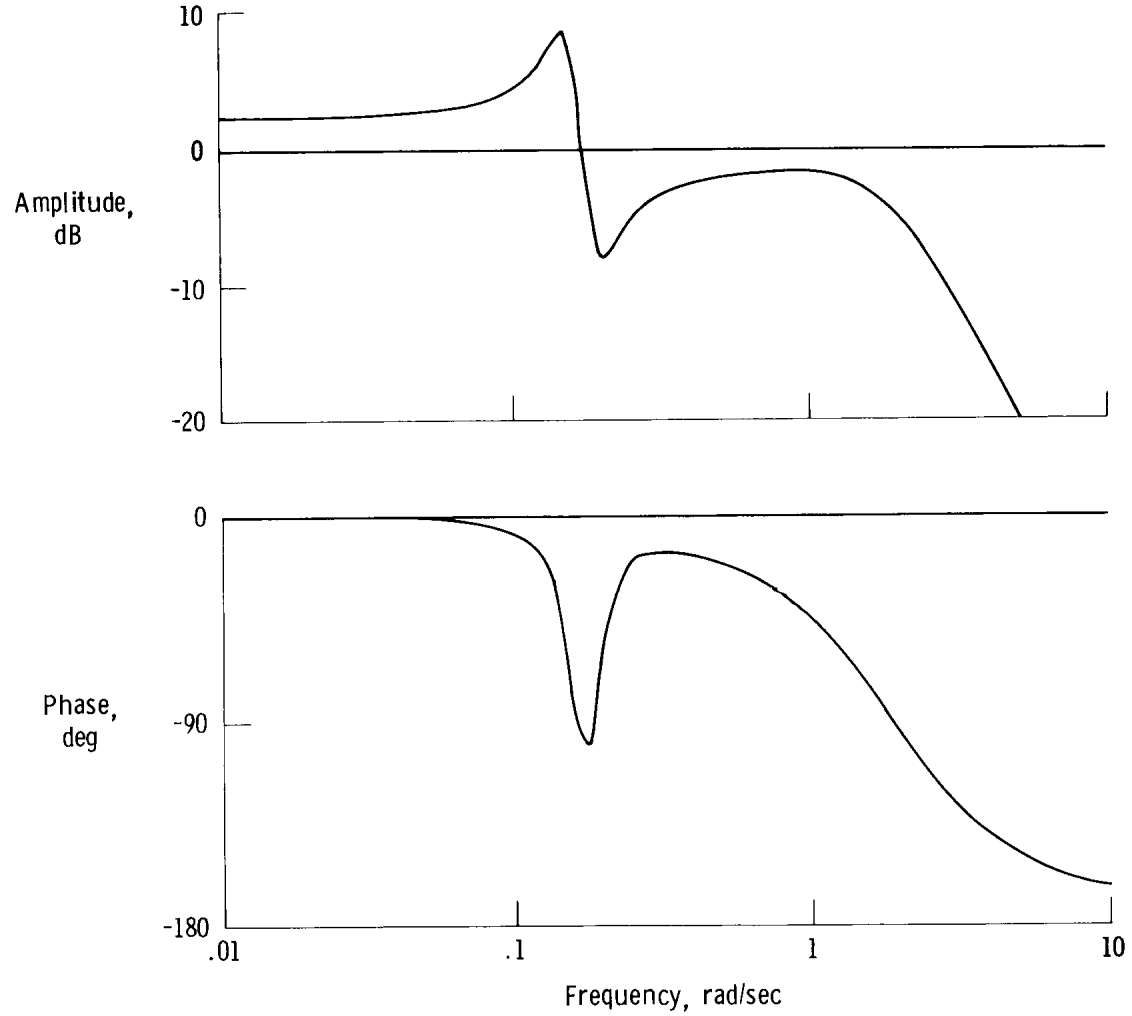

(b) Frequency response of α/δ_c.

Figure 4. Longitudinal rate feedback system.

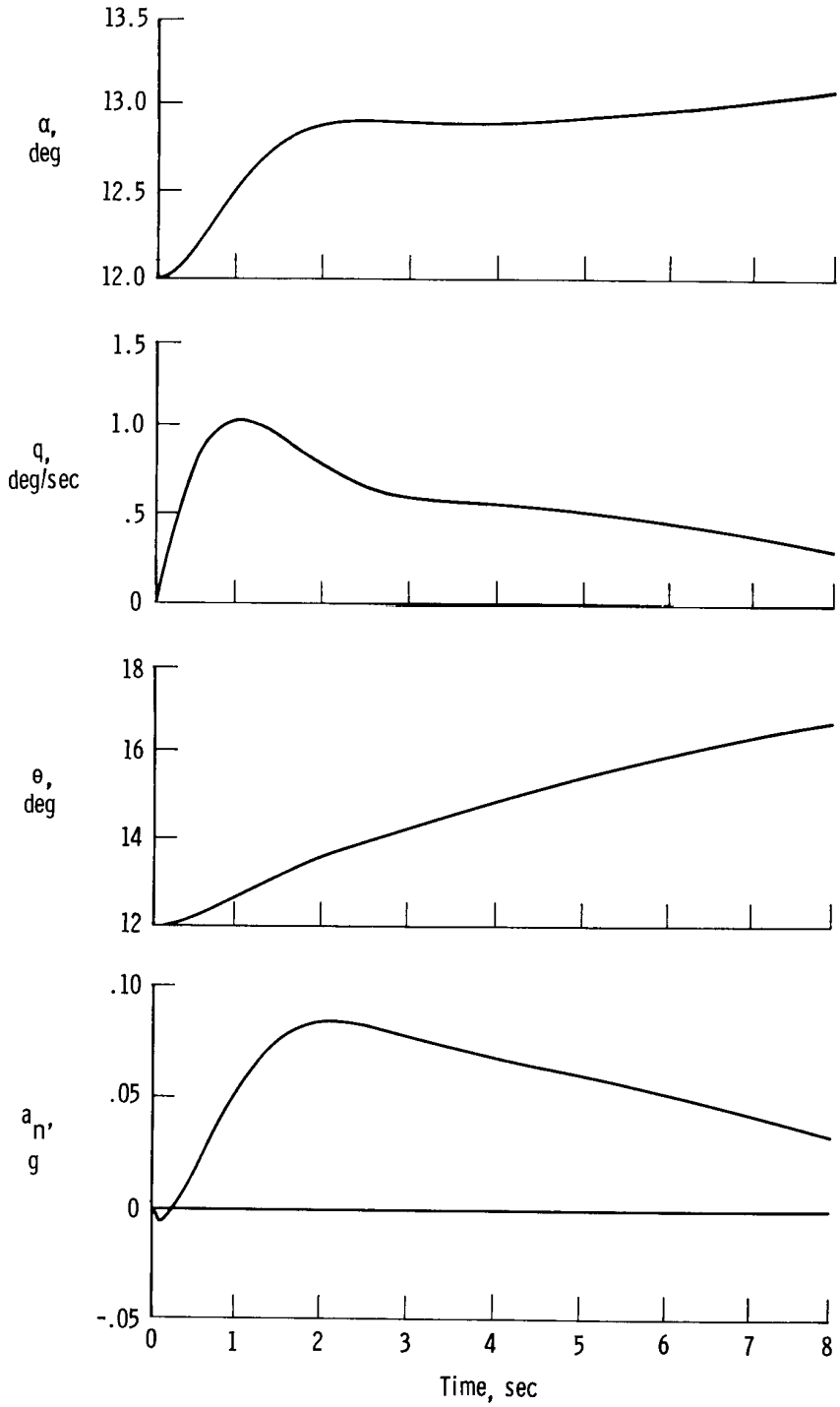

(c) Time response.

Figure 4. Concluded.

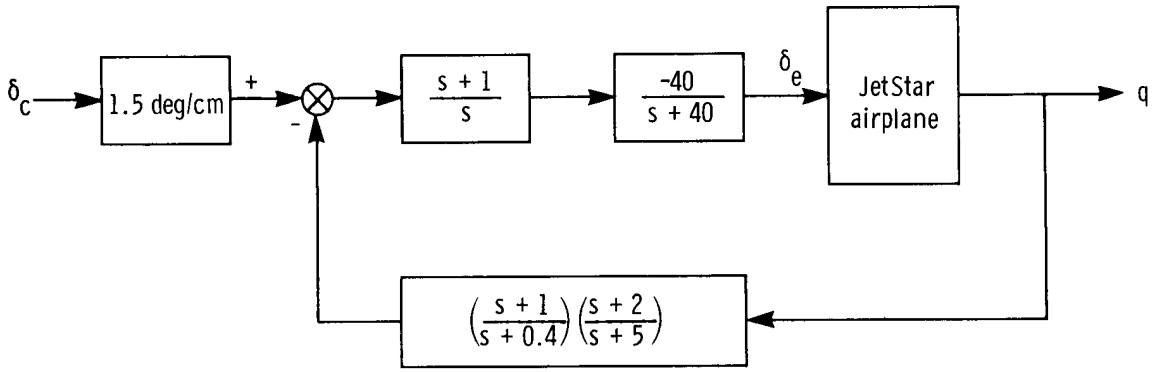

(a) Block diagram.

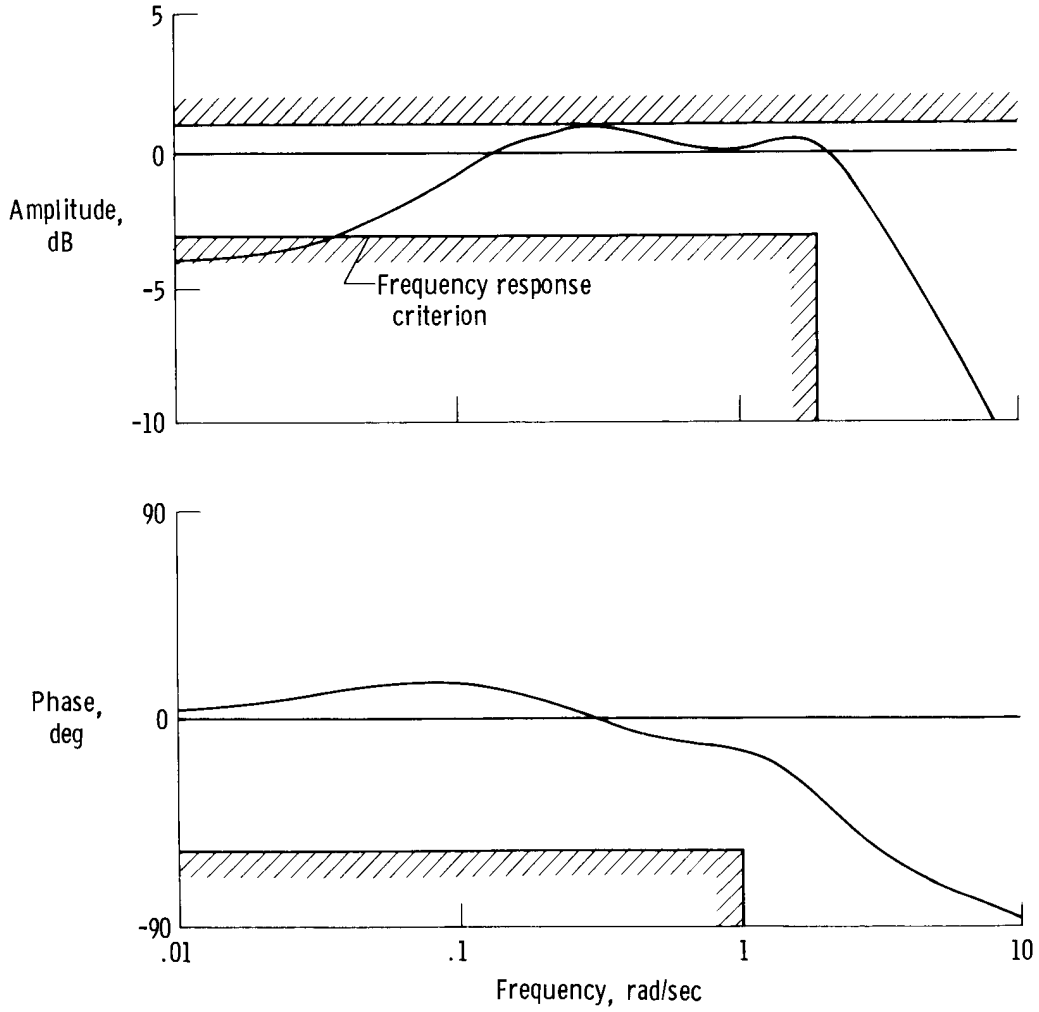

(b) Frequency response of q/δ_c.

Figure 5. Pitch rate command system.

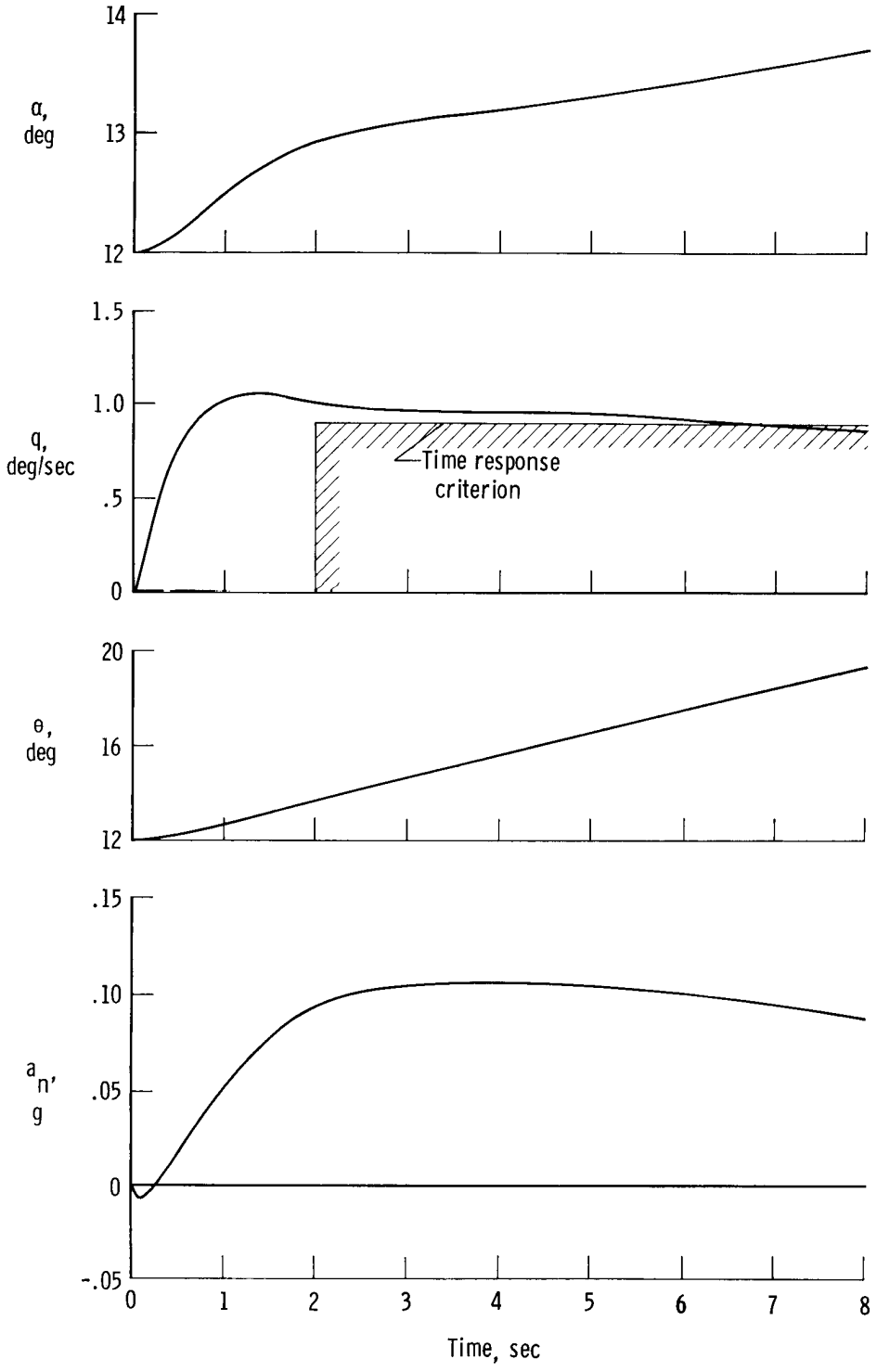

(c) Time response.

Figure 5. Concluded.

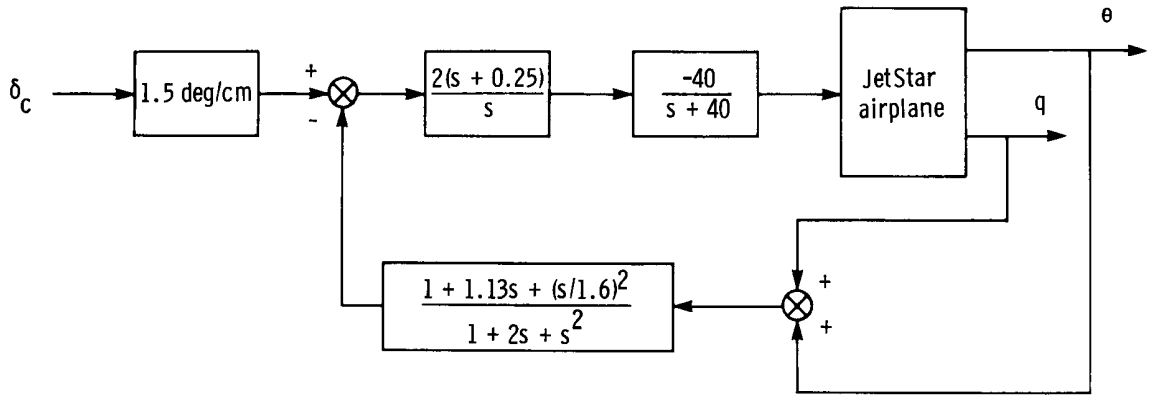

(a) Block diagram.

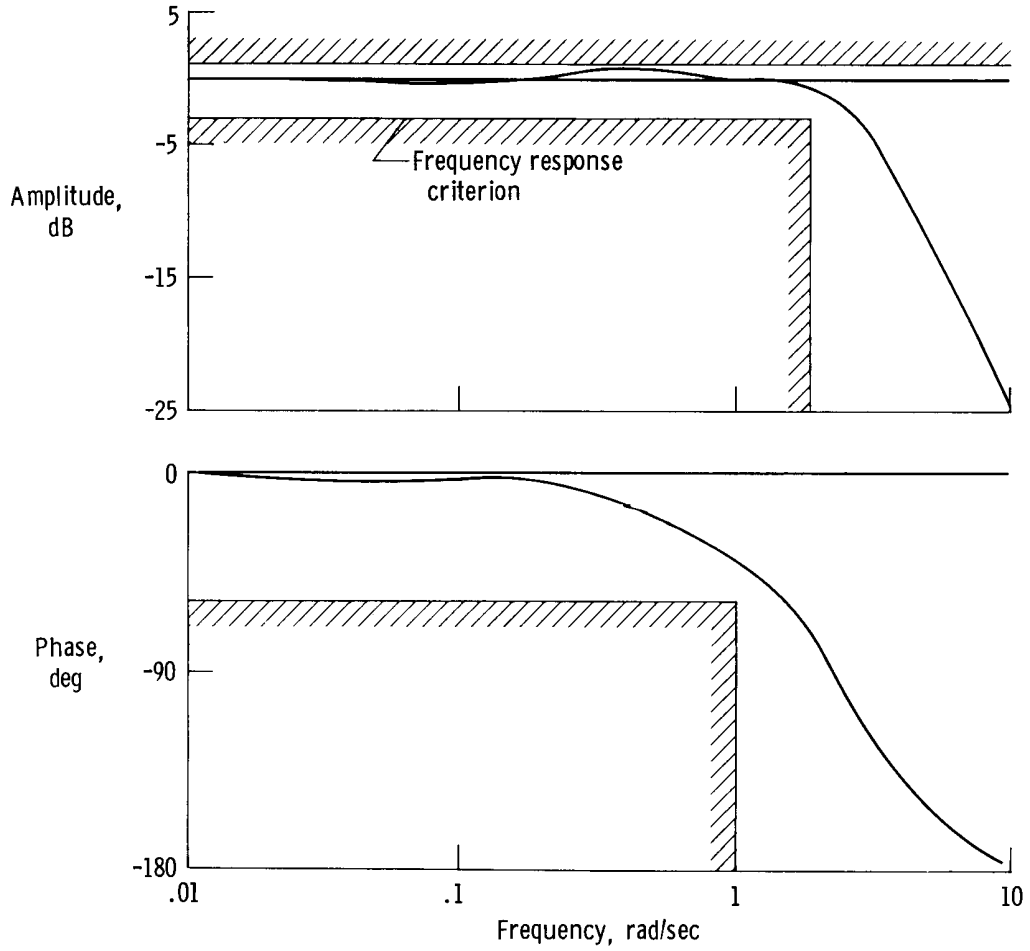

(b) Frequency response of θ/δ_c.

Figure 6. Pitch attitude command system.

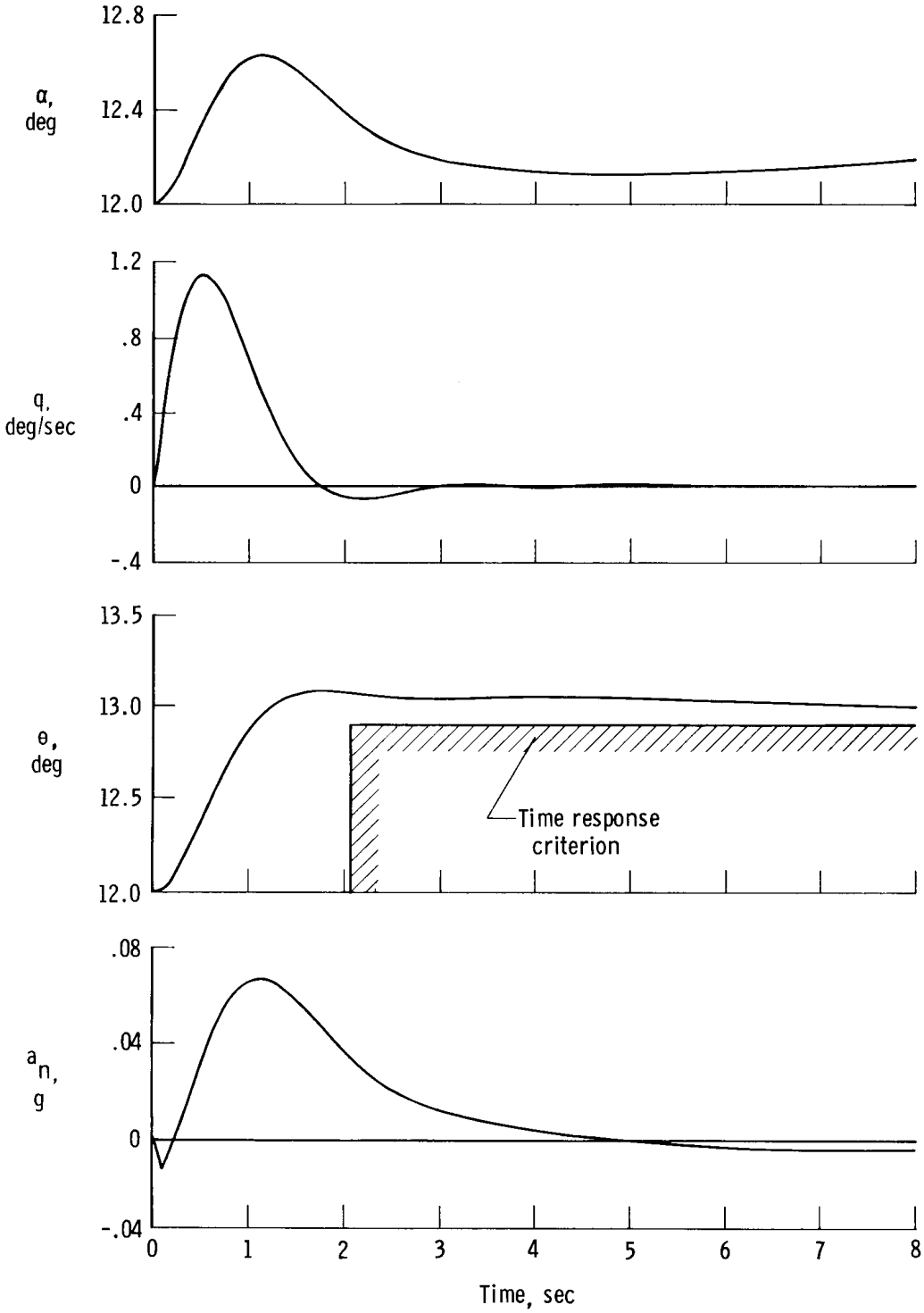

(c) Time response.

Figure 6. Concluded.

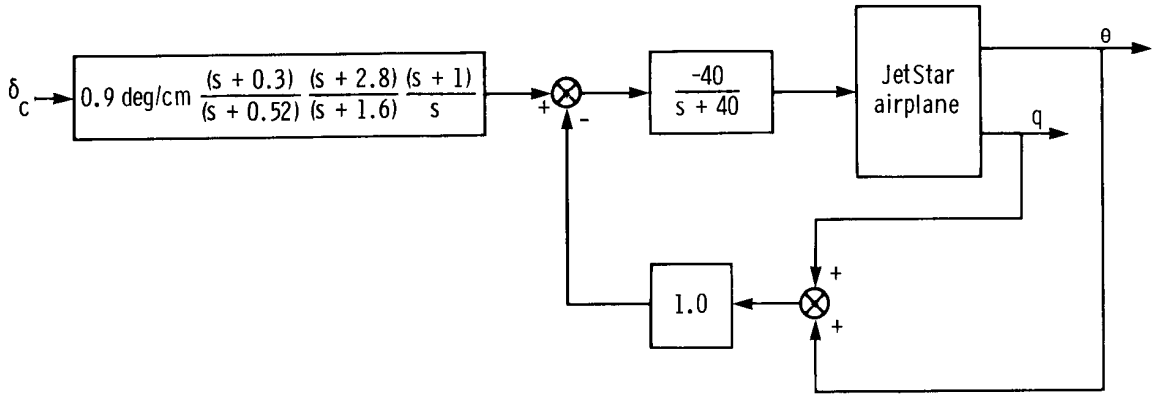

(a) Block diagram.

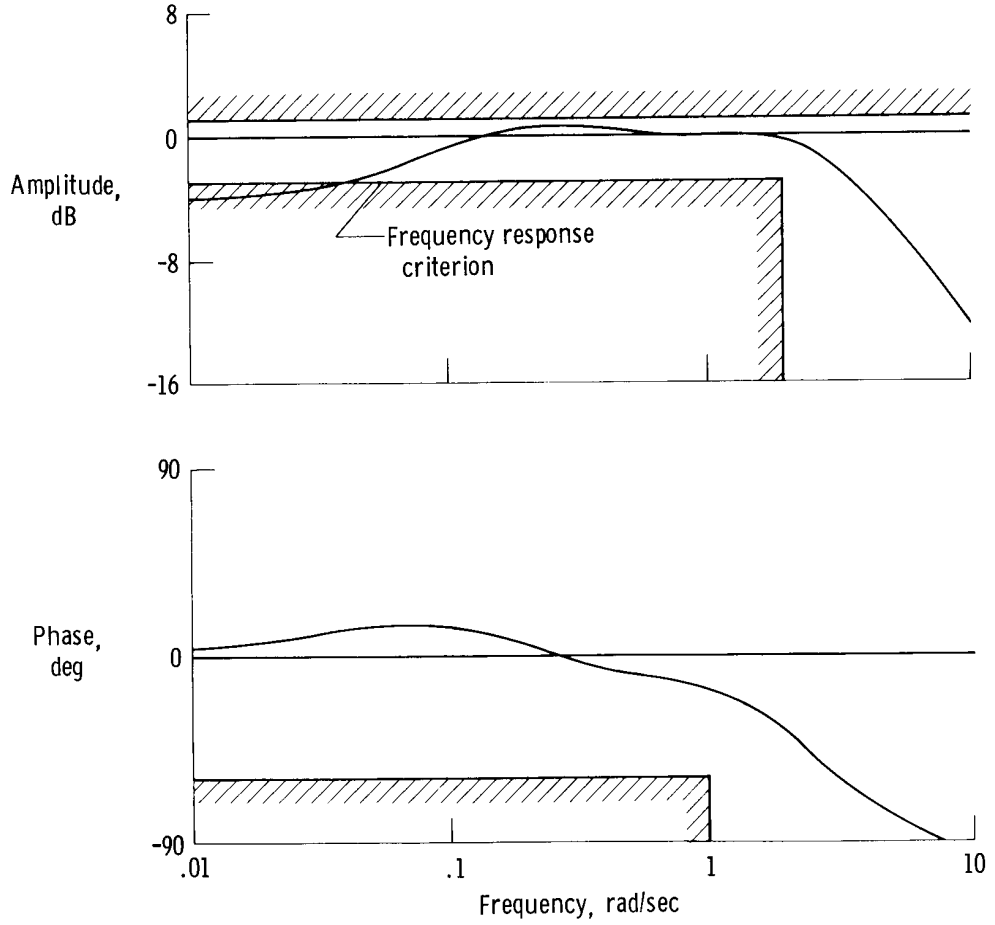

(b) Frequency response of q/δ_c.

Figure 7. Pitch rate command/attitude hold system.

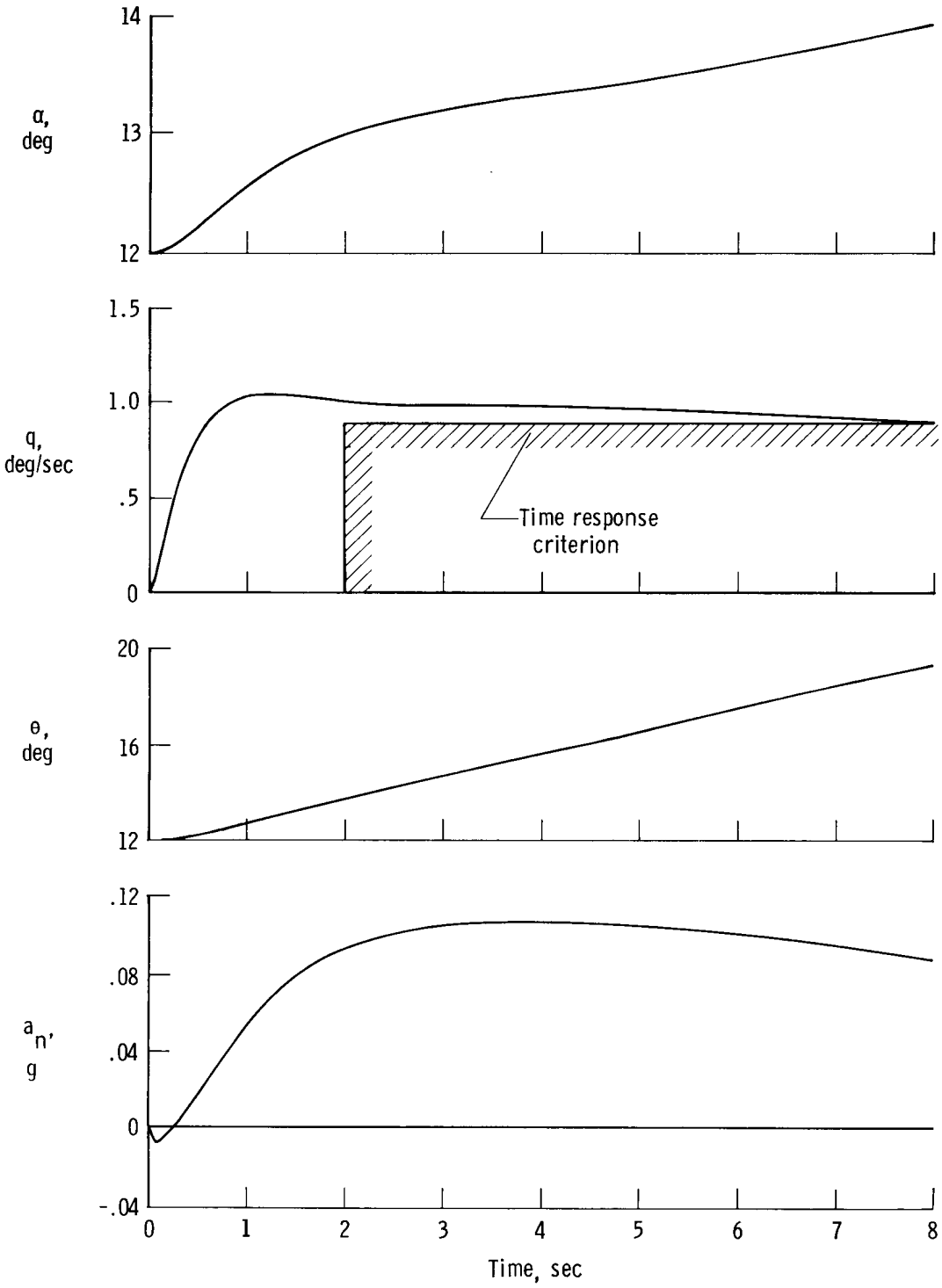

(c) Time response.

Figure 7. Concluded.

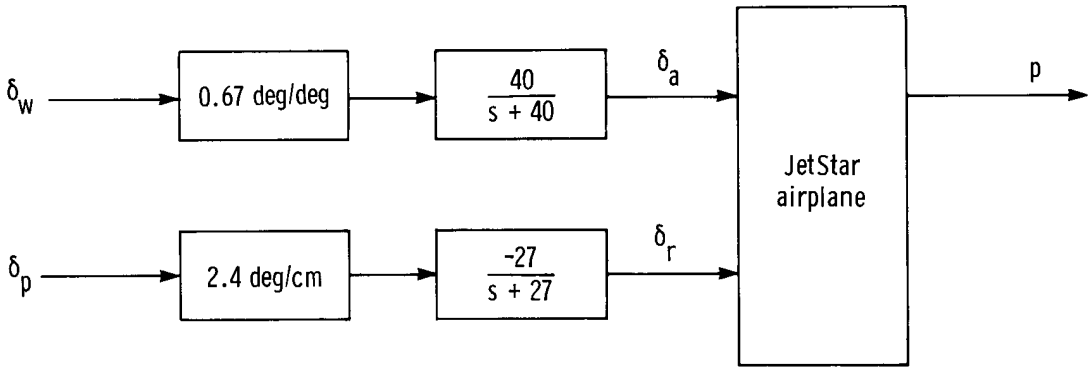

(a) Block diagram.

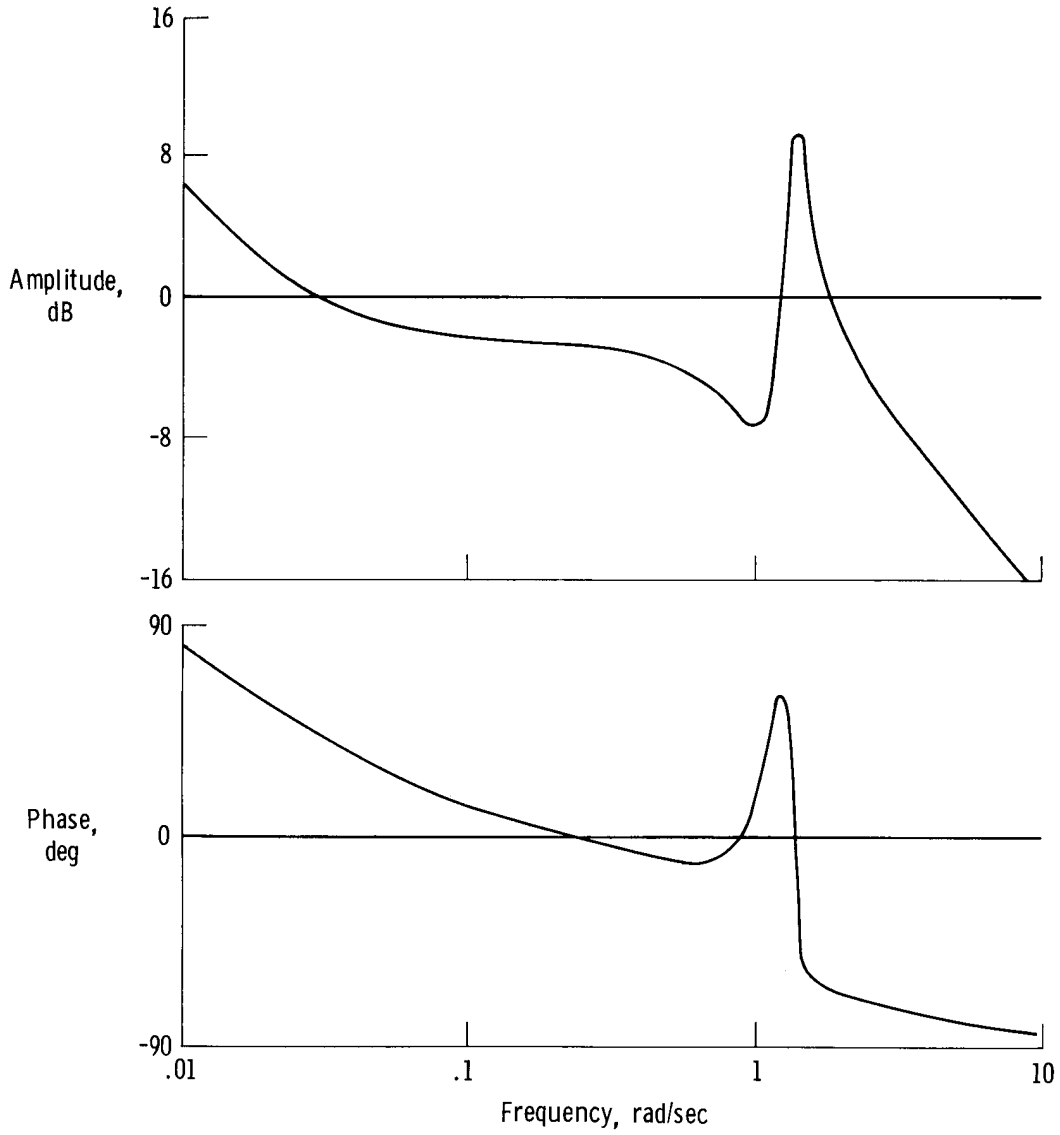

(b) Frequency response of p/δ_w.

Figure 8. Basic lateral-directional system.

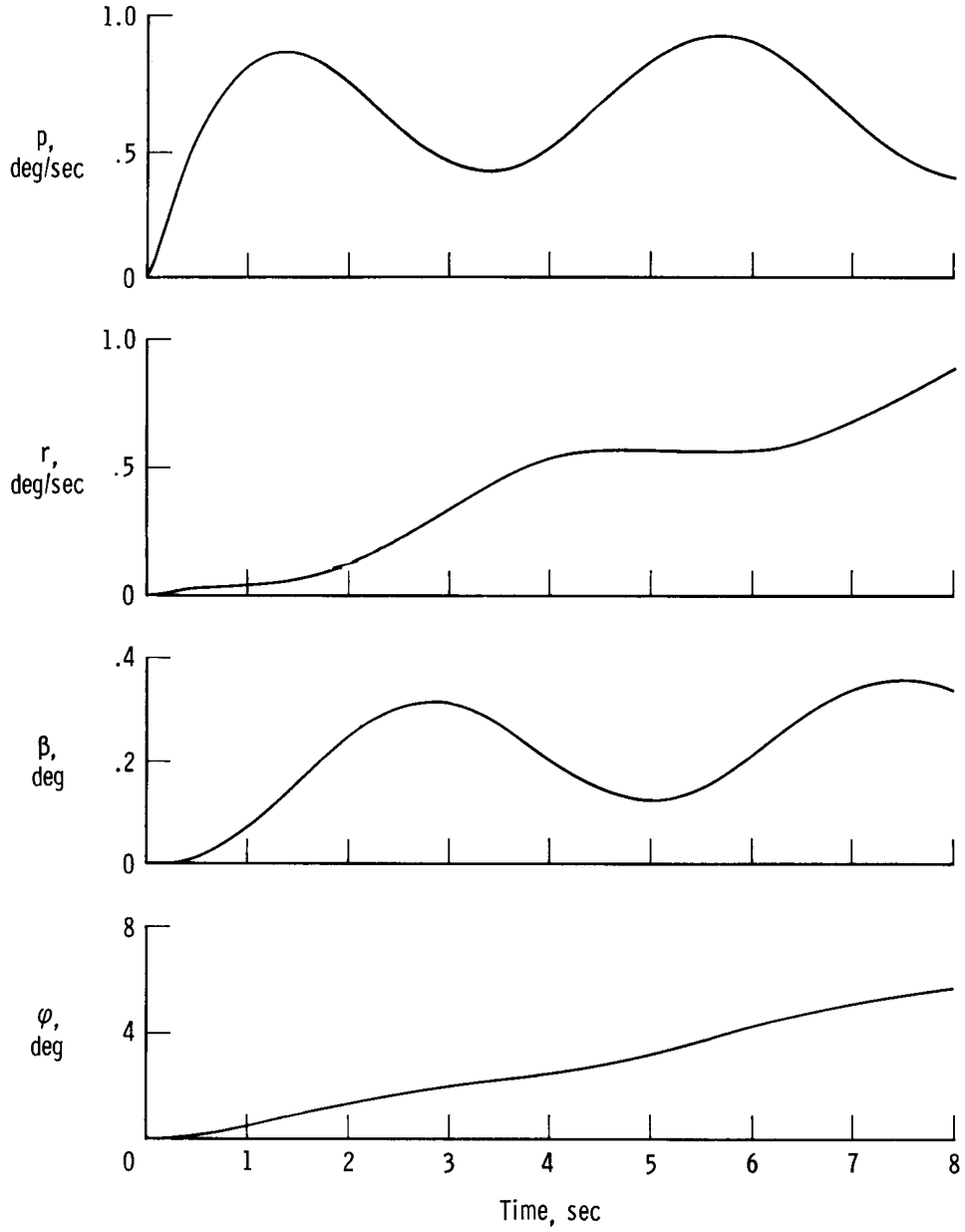

(c) Time response.

Figure 8. Concluded.

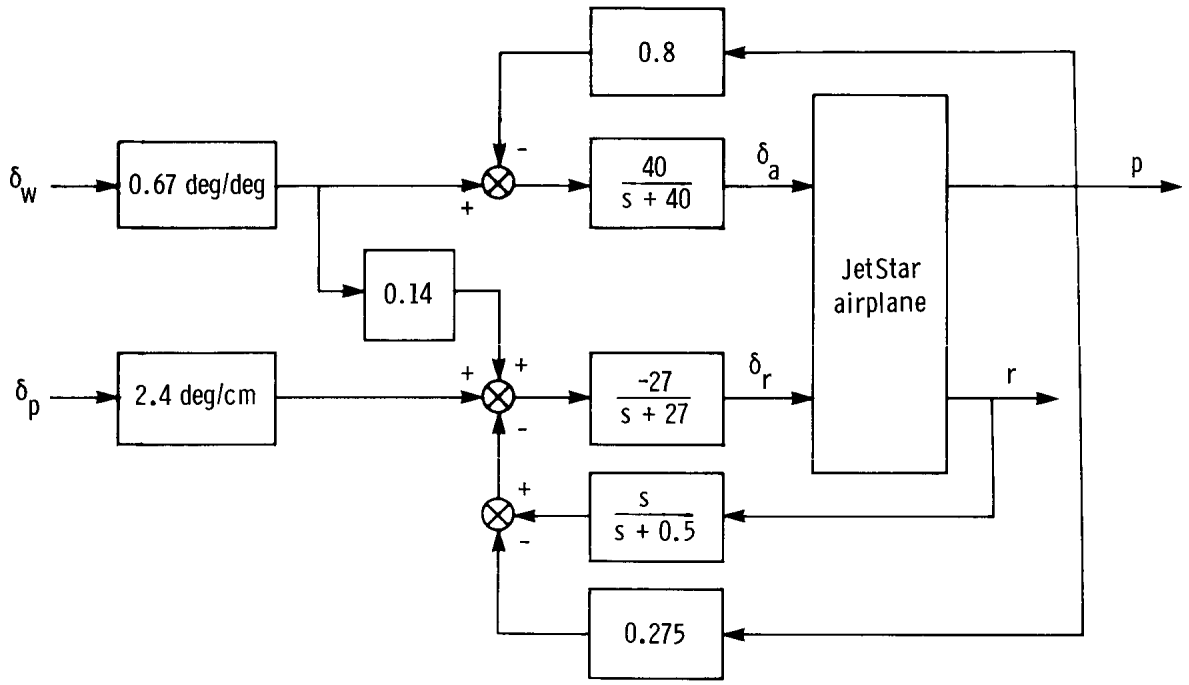

(a) Block diagram.

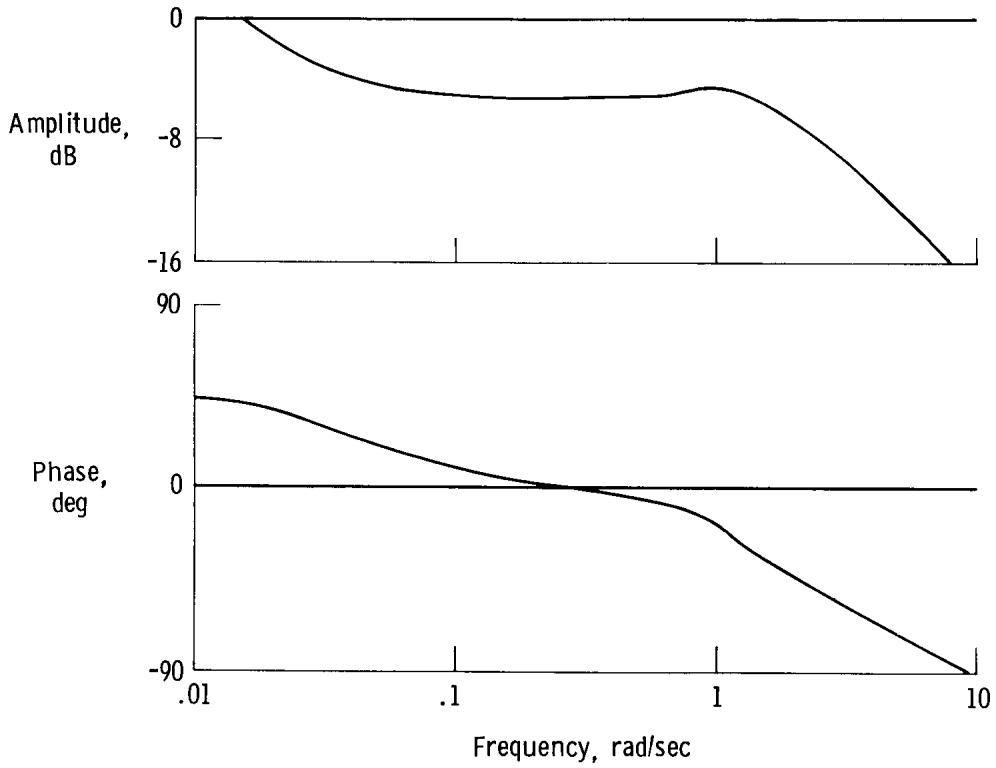

(b) Frequency response of p/δ_w.

Figure 9. Lateral-directional rate feedback system.

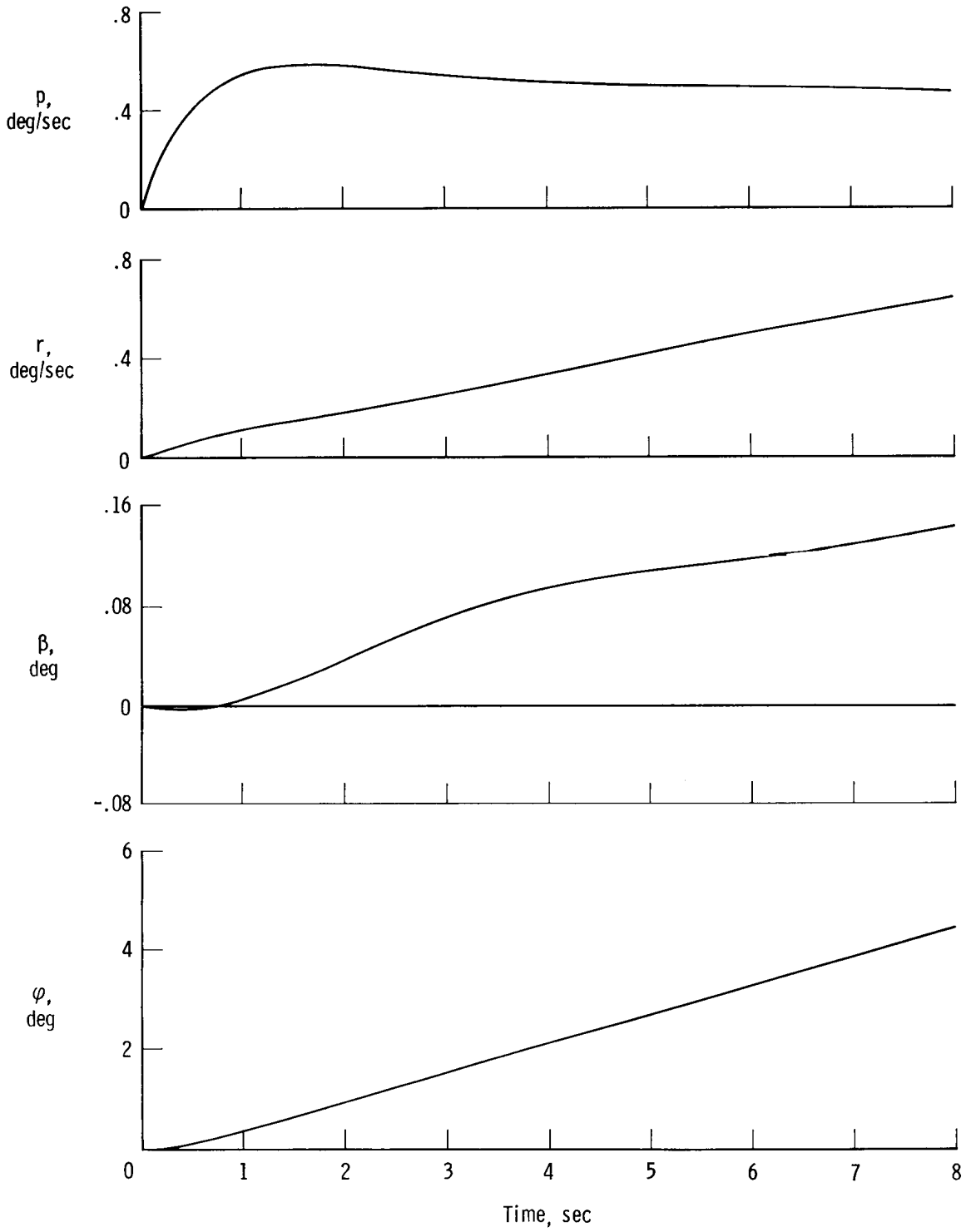

(c) Time response.

Figure 9. Concluded.

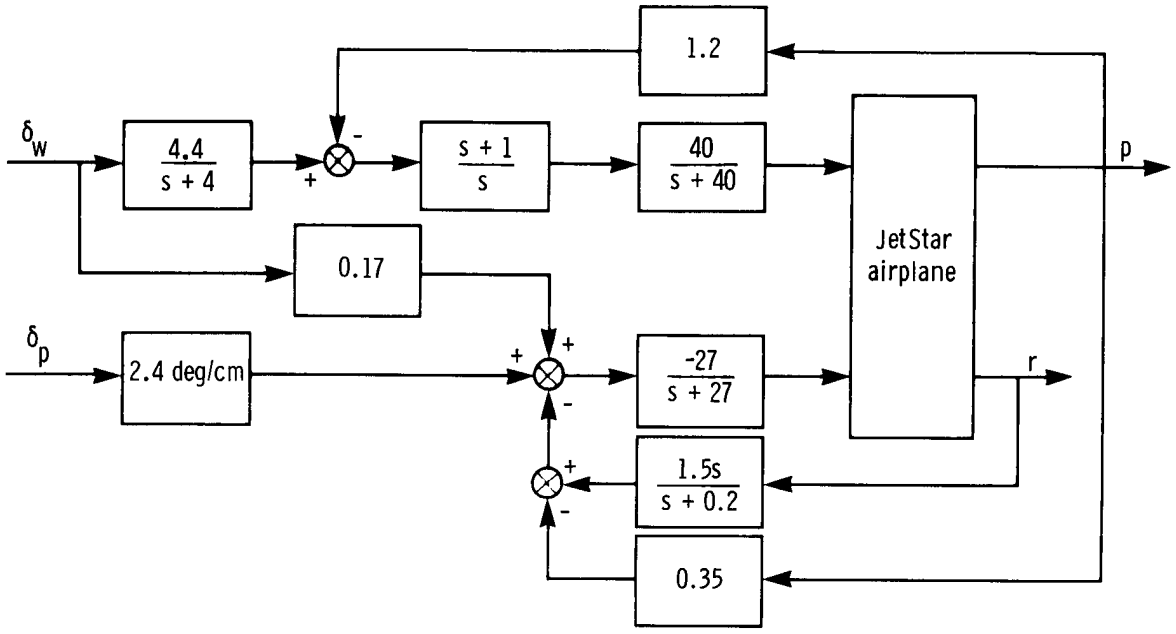

(a) Block diagram.

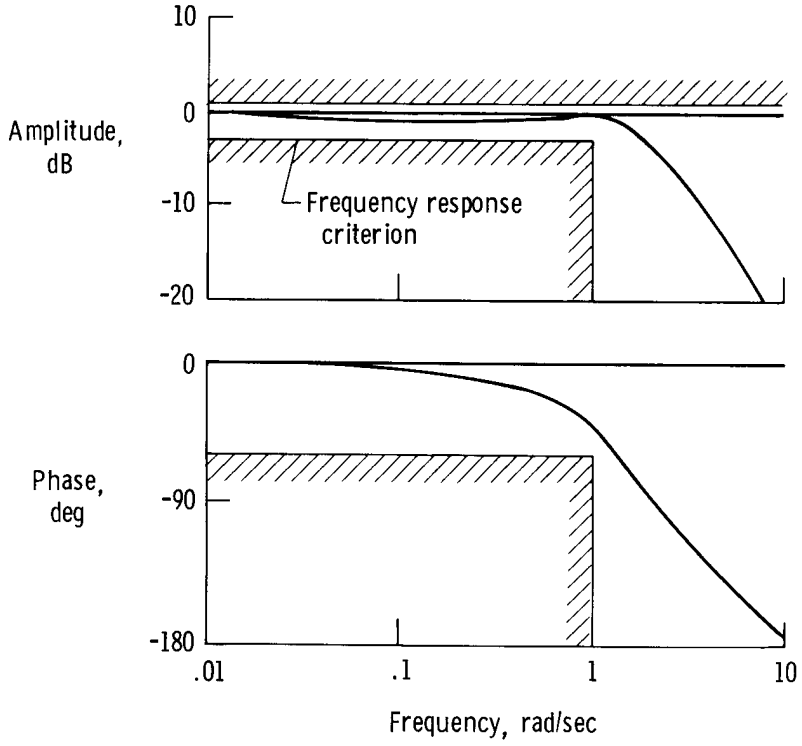

(b) Frequency response of p/δ_w.

Figure 10. Roll rate command system.

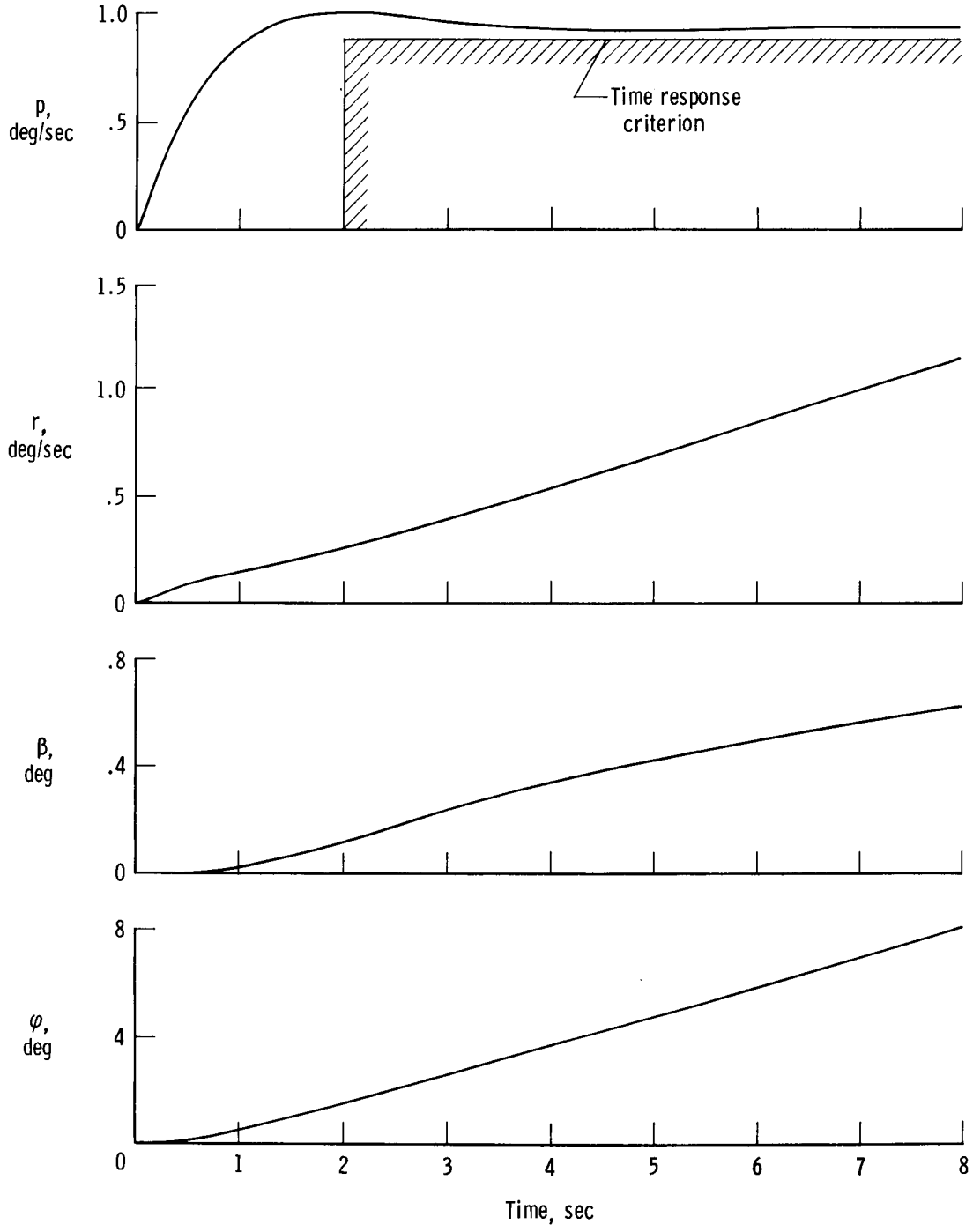

(c) Time response.

Figure 10. Concluded.

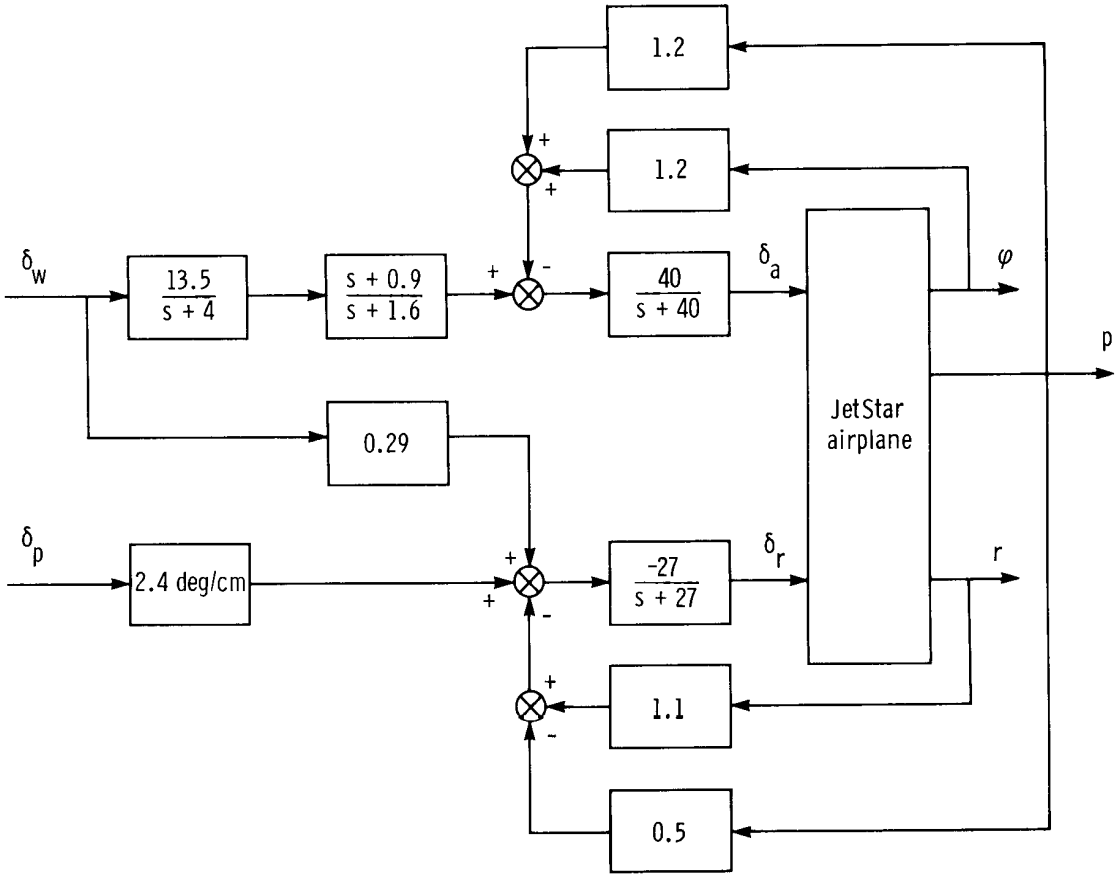

(a) Block diagram.

Figure 11. Roll attitude command system.

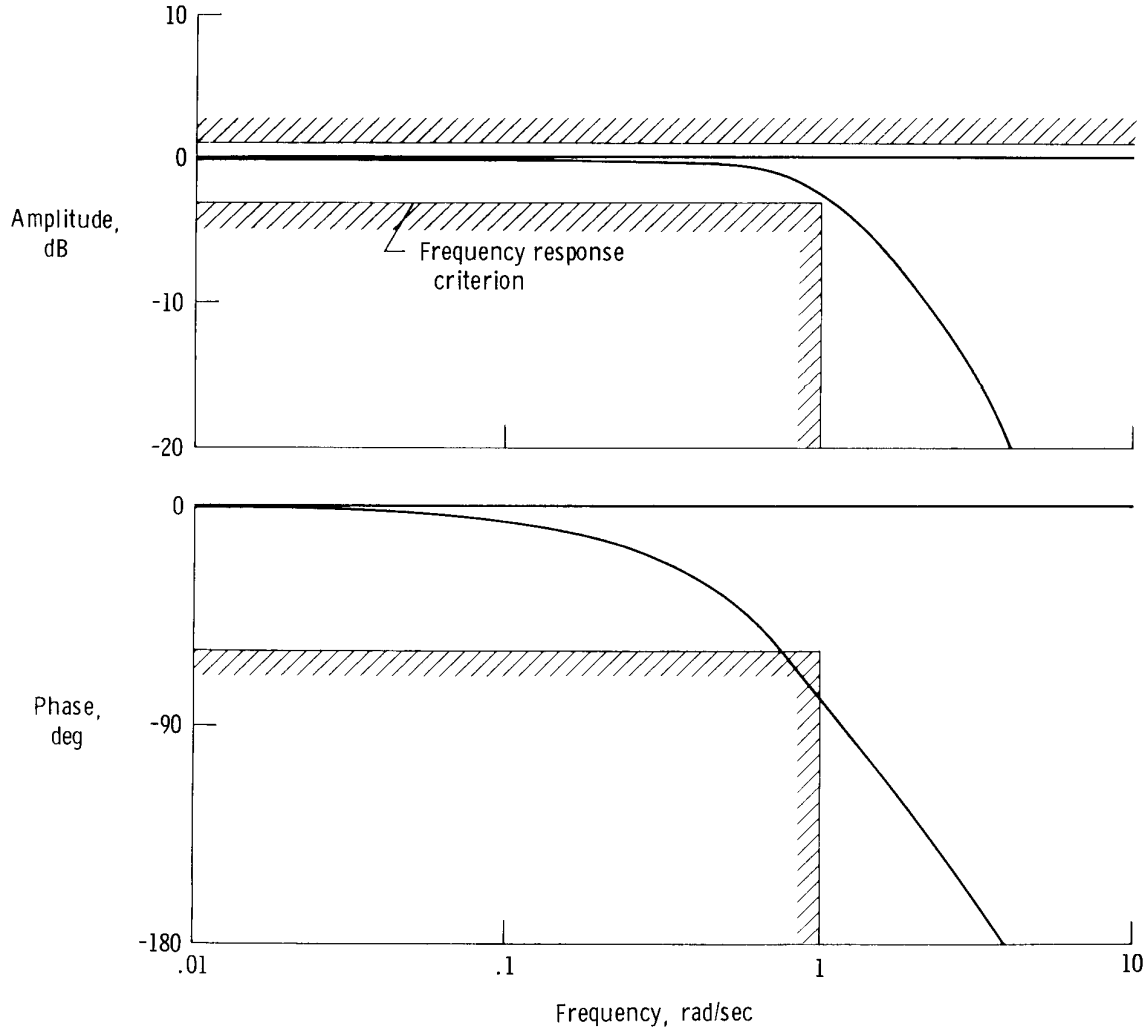

(b) Frequency response of φ/δ_w.

Figure 11. Continued.

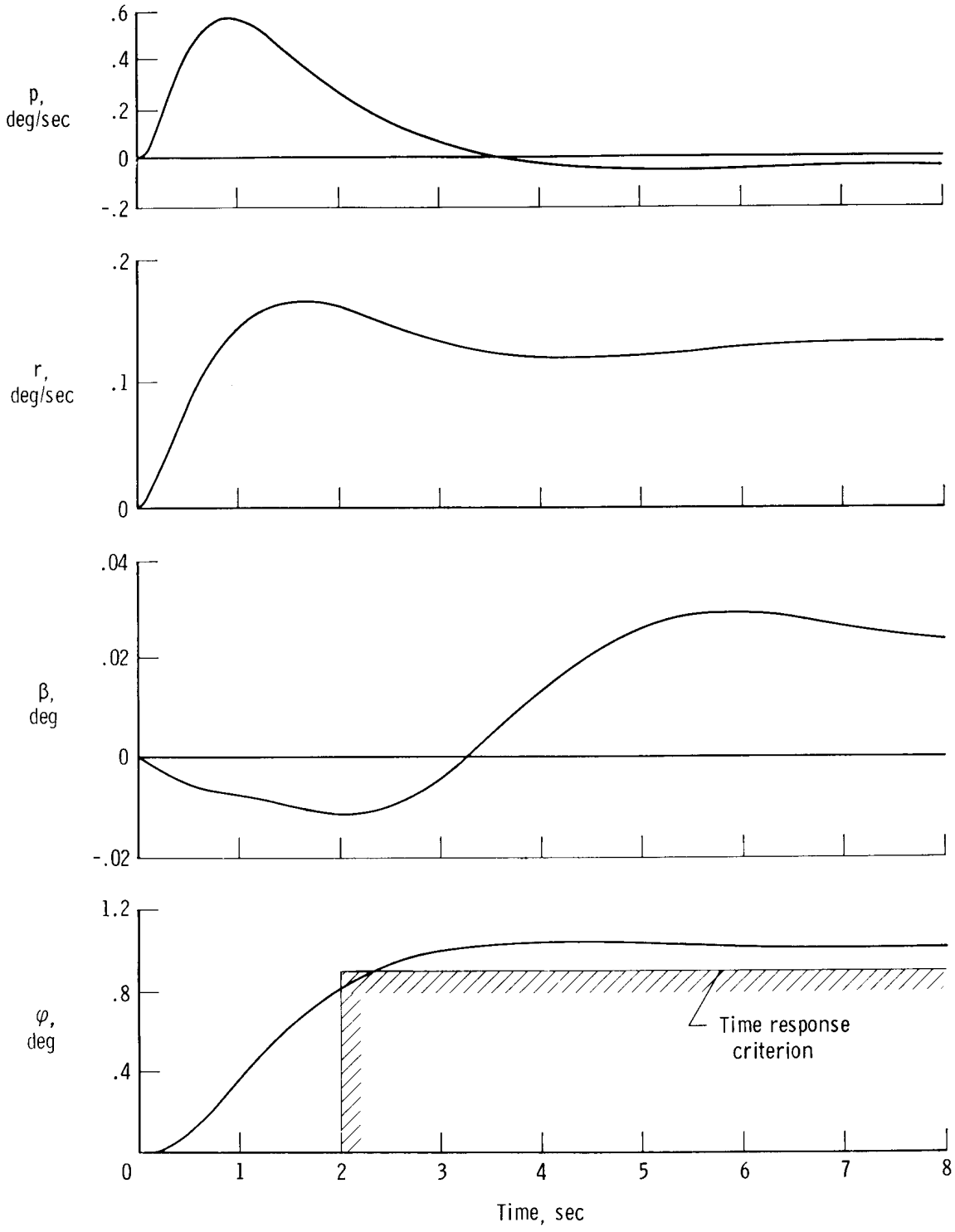

(c) Time response.

Figure 11. Concluded.

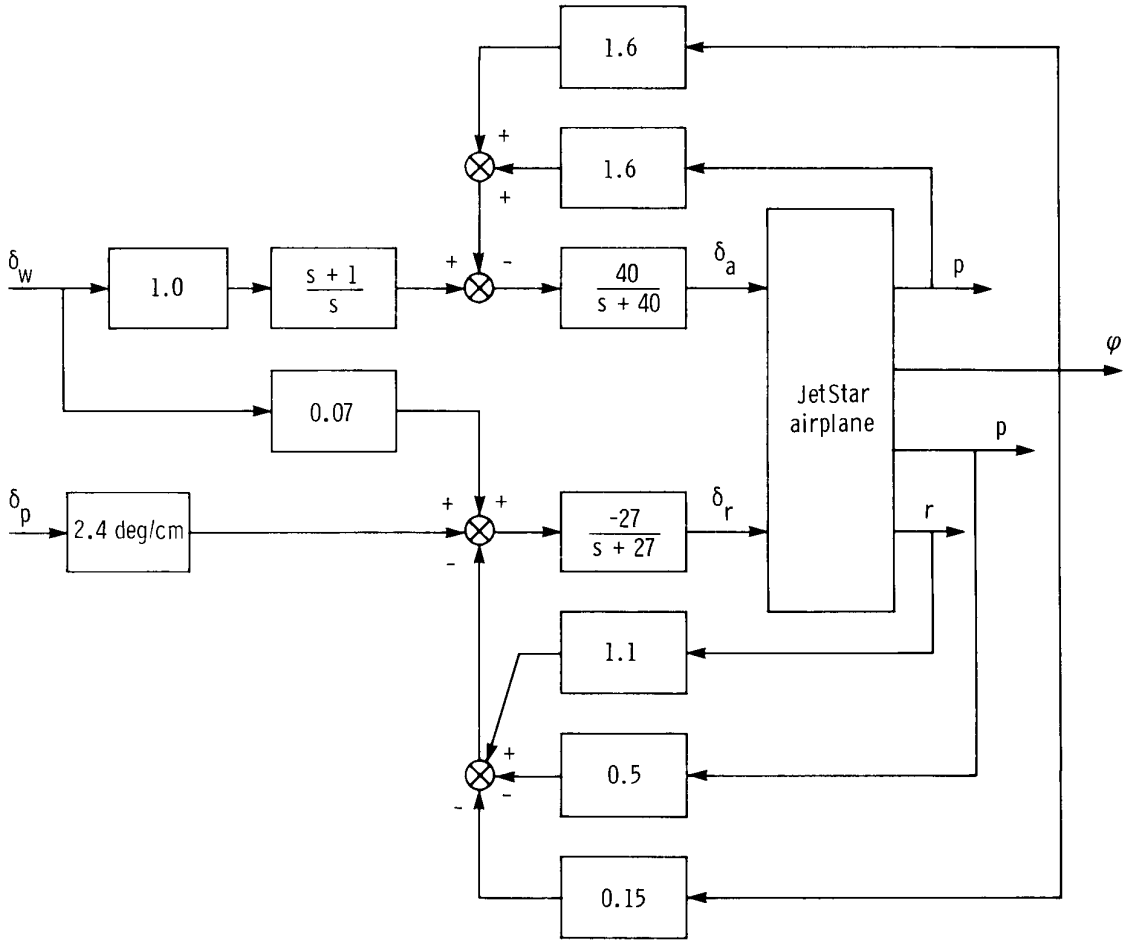

(a) Block diagram.

Figure 12. Roll rate command/attitude hold system.

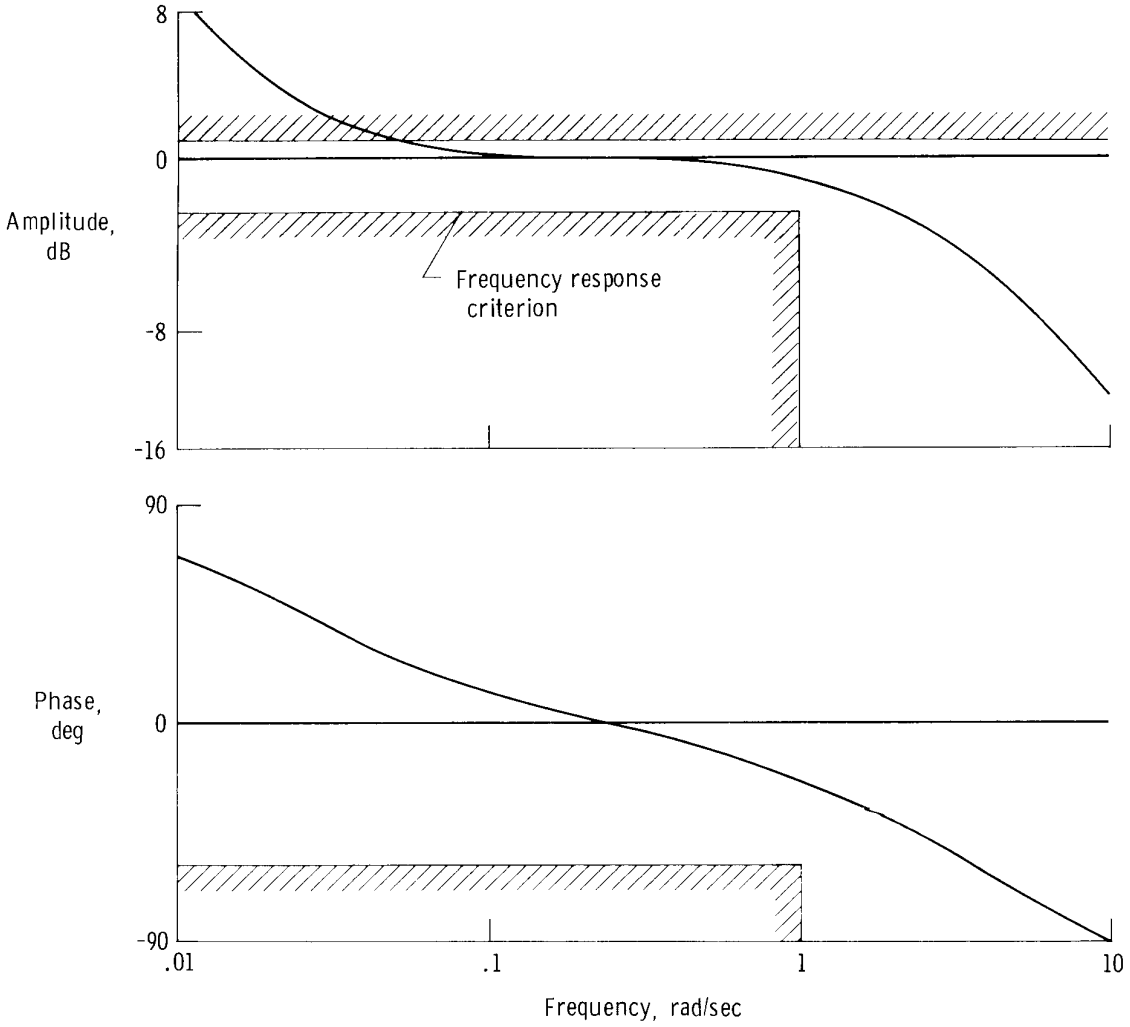

(b) Frequency response of p/δ_w.

Figure 12. Continued.

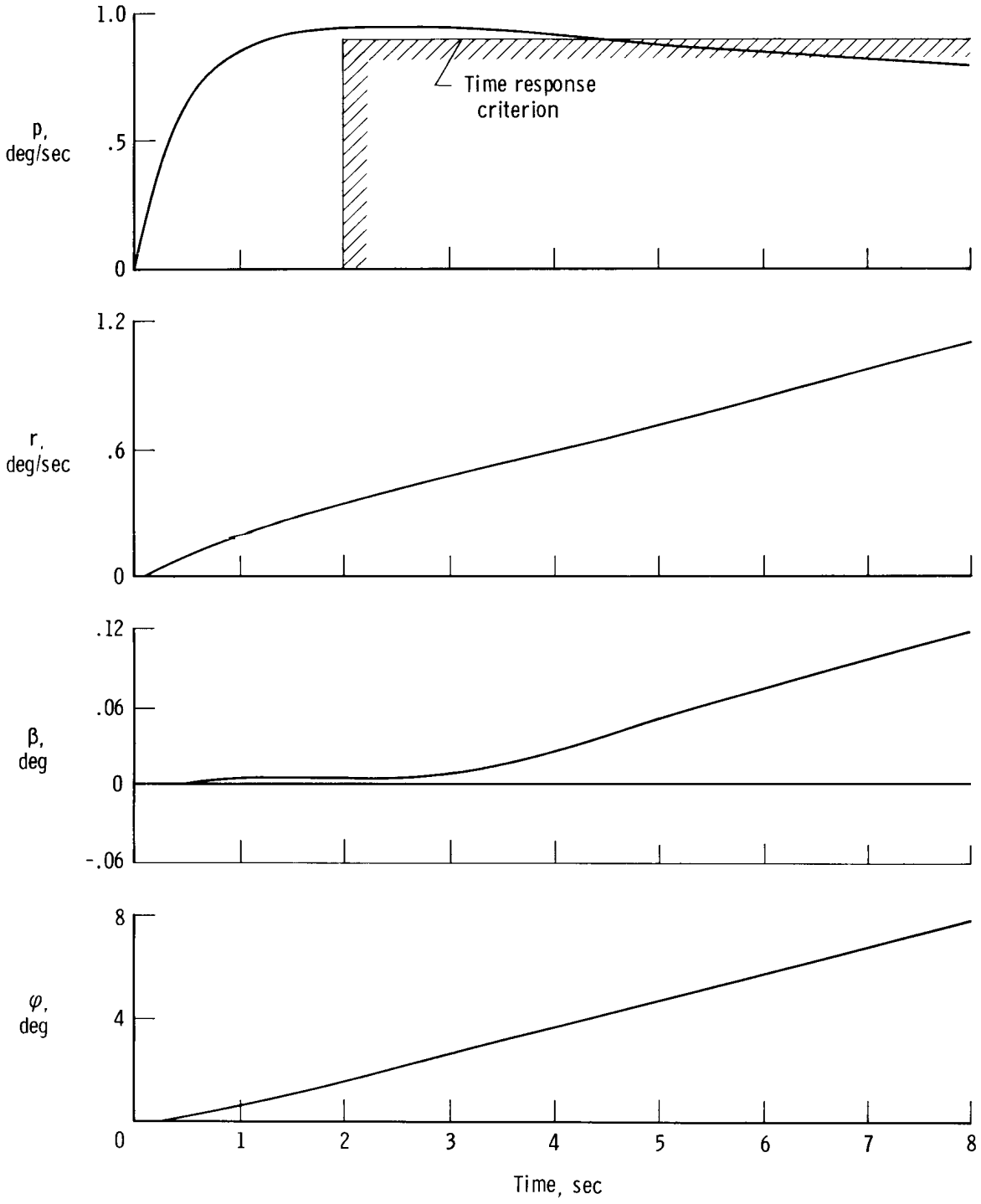

(c) Time response.

Figure 12. Concluded.

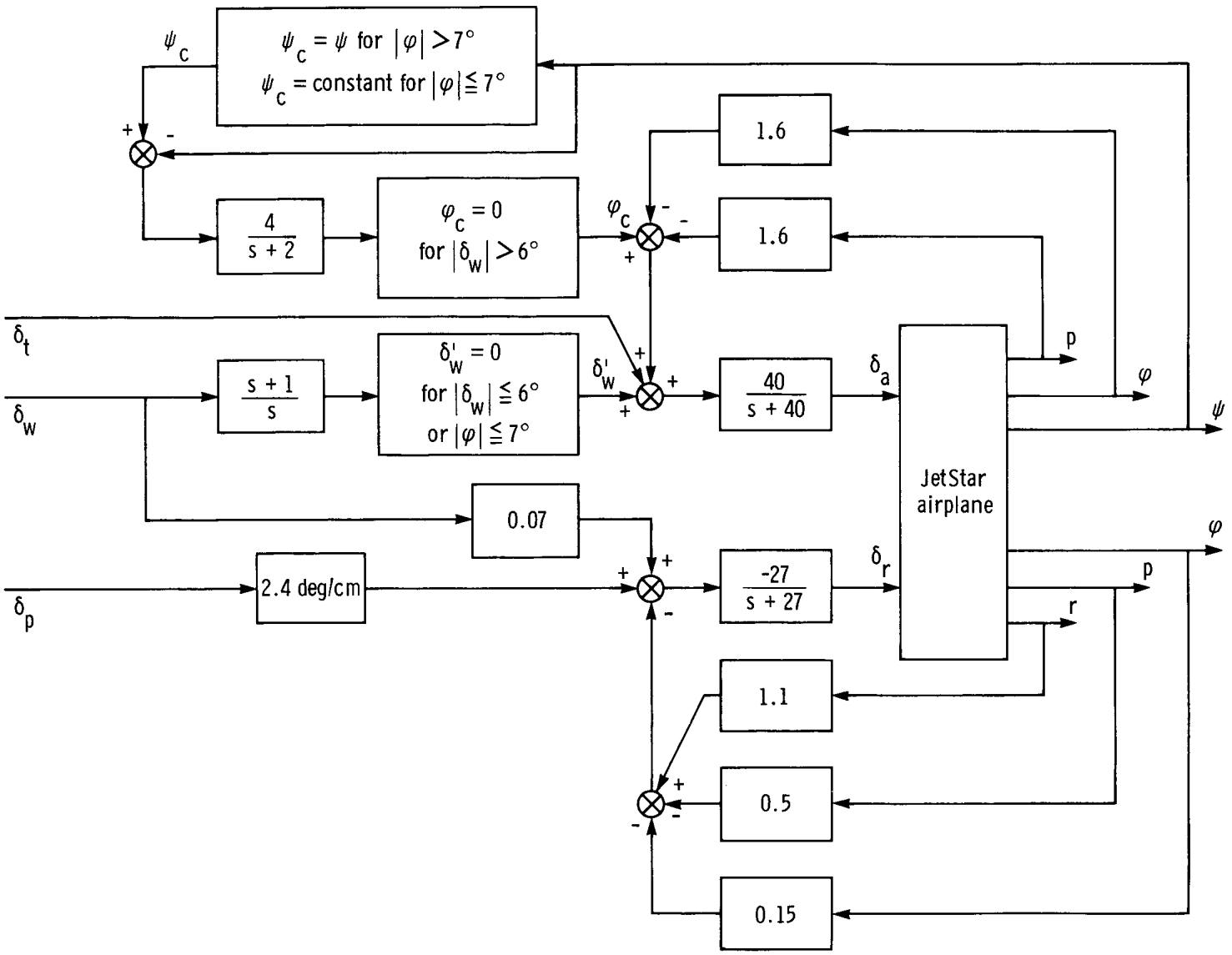

(a) Block diagram.

Figure 13. Control wheel steering system.

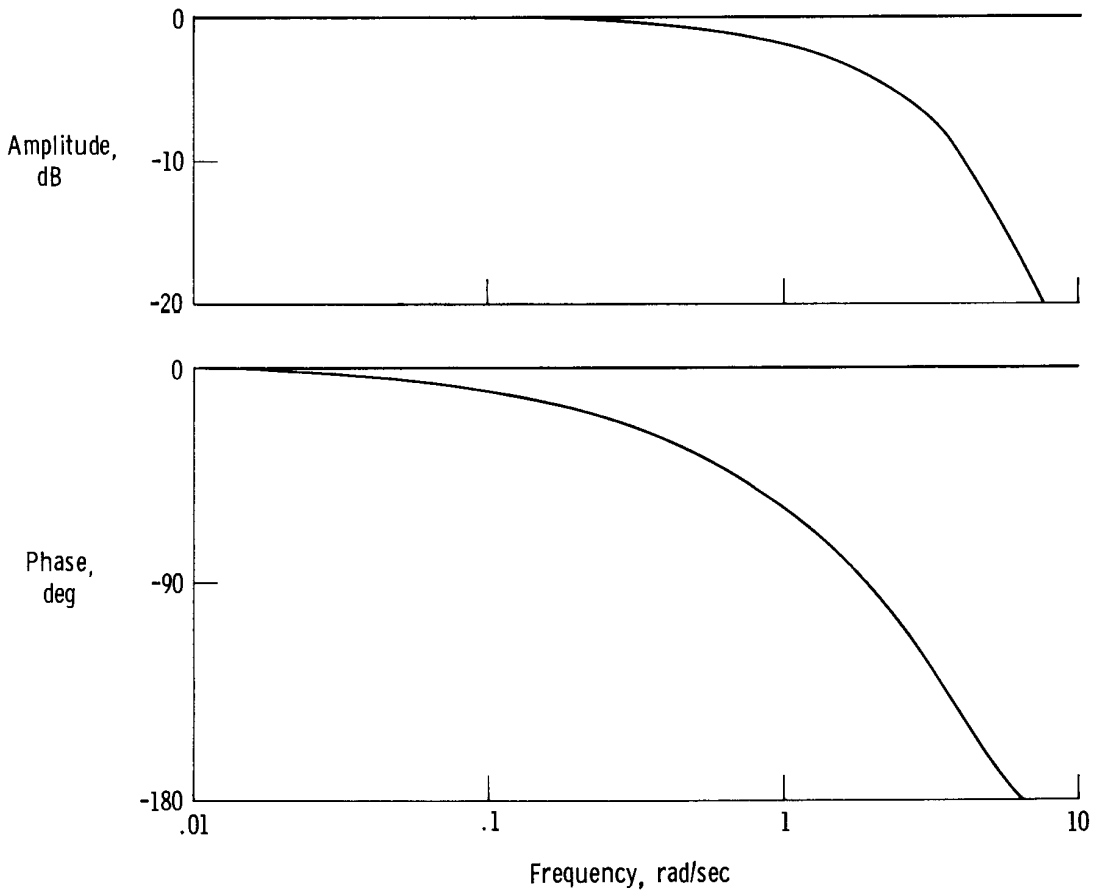

(b) Frequency response of ψ/δ_t.

Figure 13. Continued.

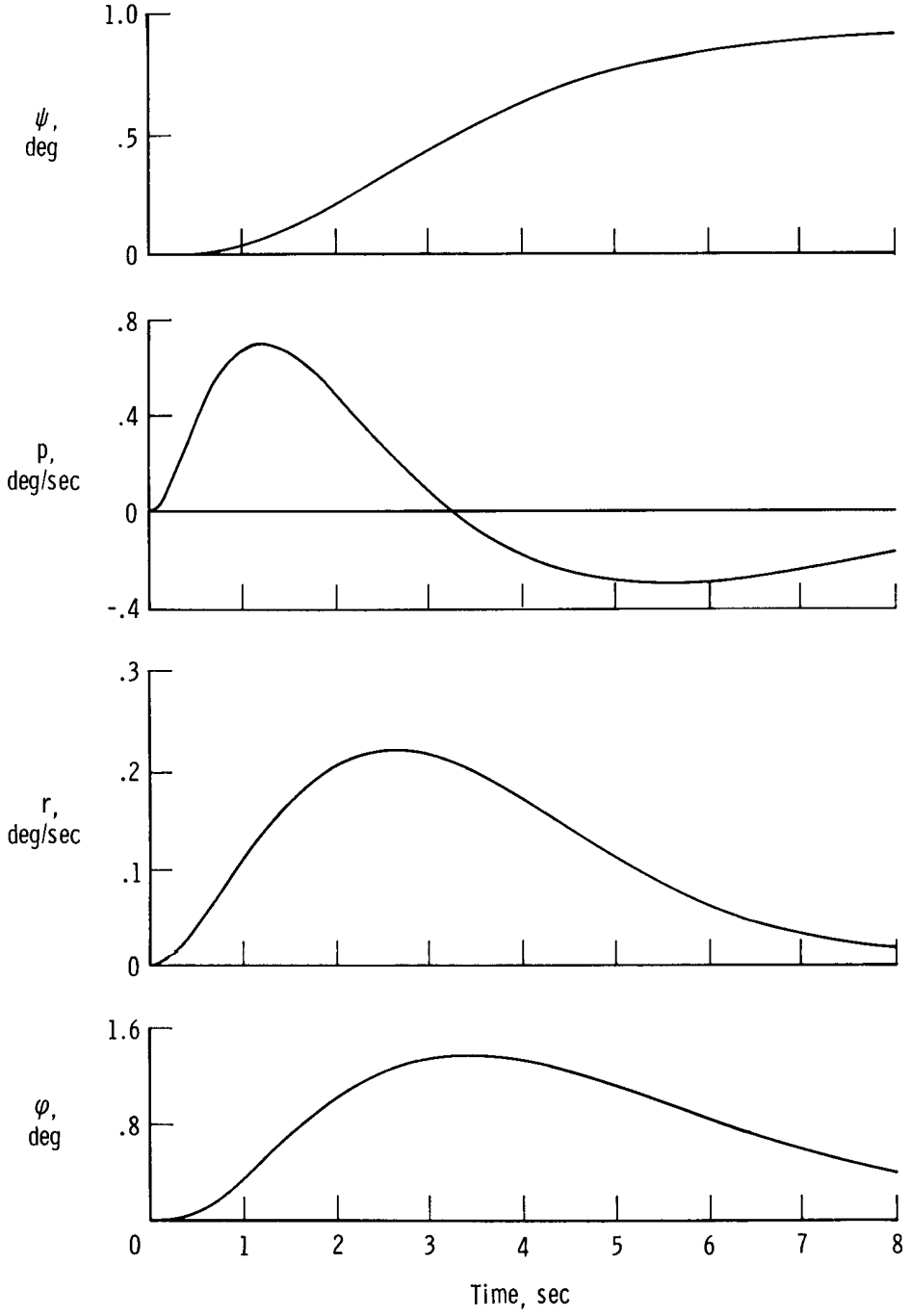

(c) Time response.

Figure 13. Concluded.

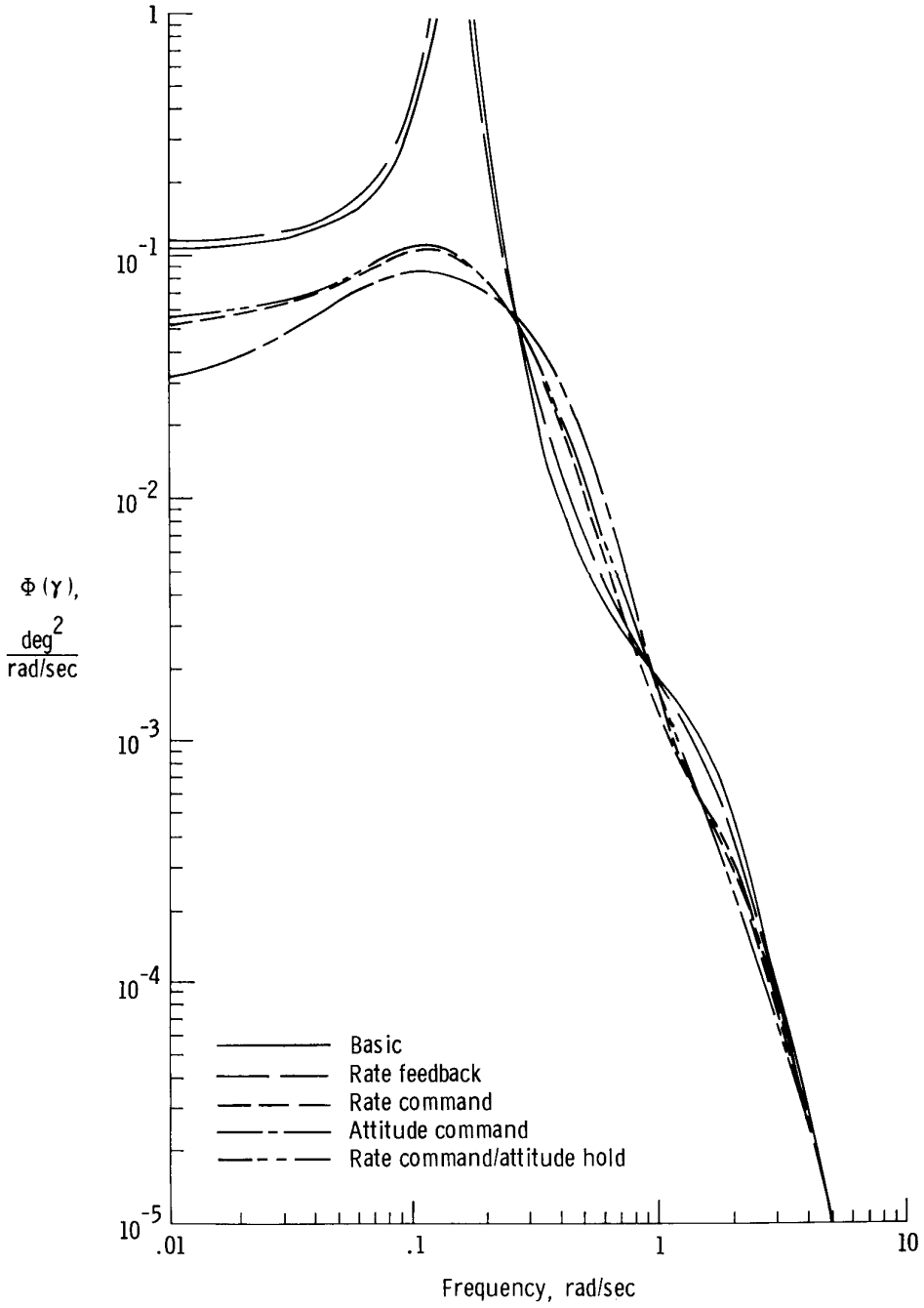

(a) Flightpath angle.

Figure 14. Effect of control law configuration on power spectral densities for a 0.3-meter-per-second rms turbulence input.

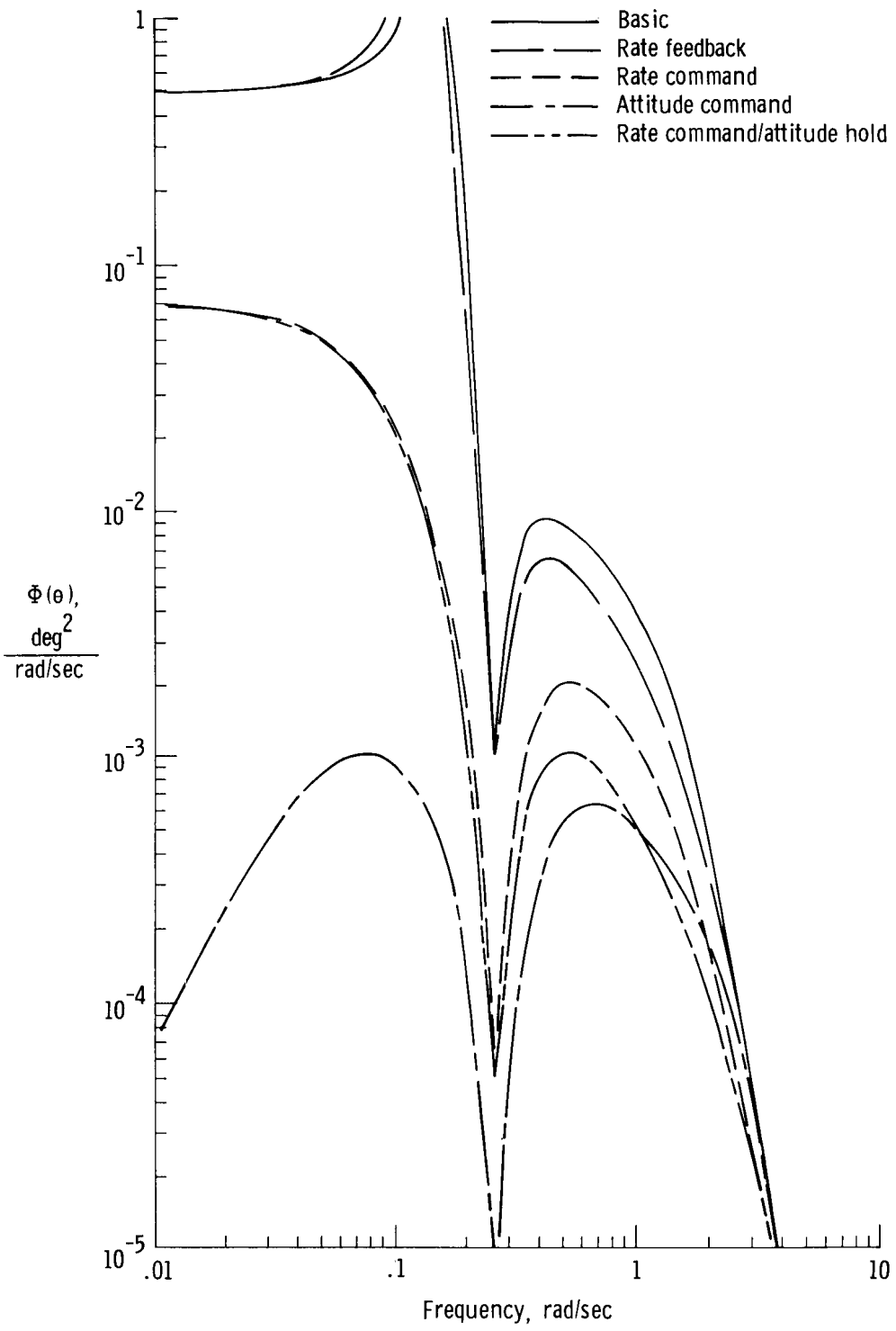

(b) Pitch angle.

Figure 14. Continued.

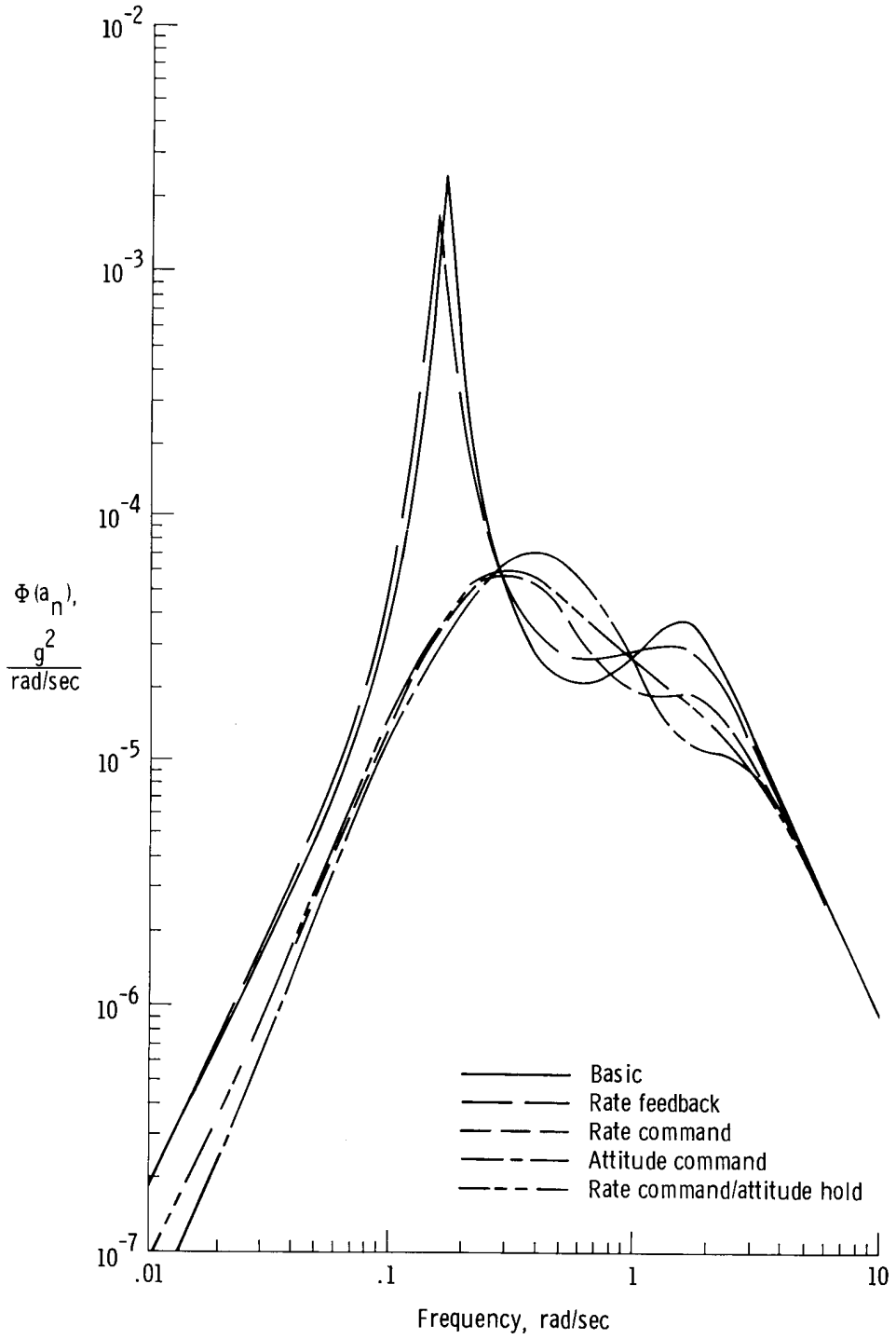

(c) Normal acceleration.

Figure 14. Continued.

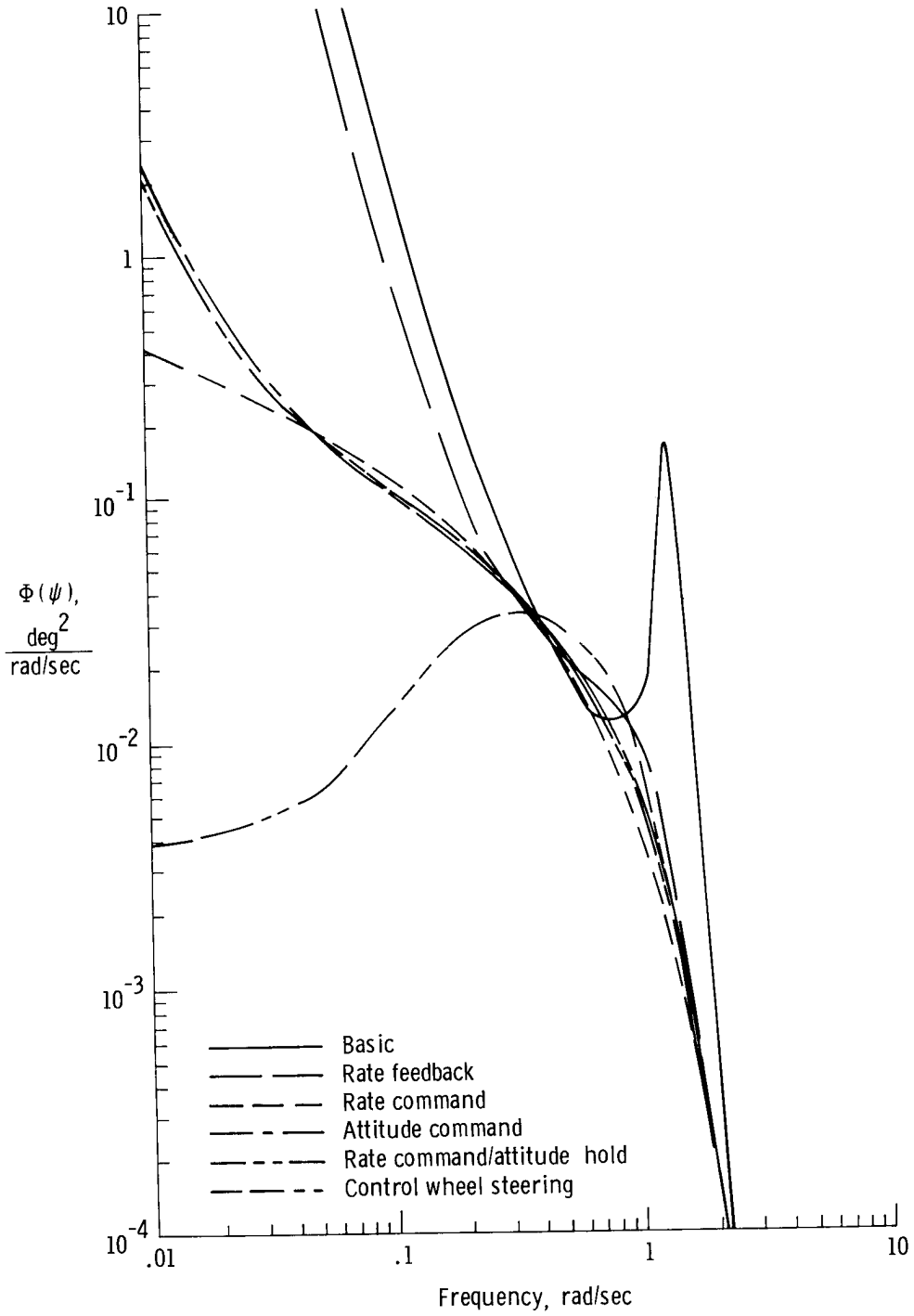

(d) Heading angle.

Figure 14. Continued.

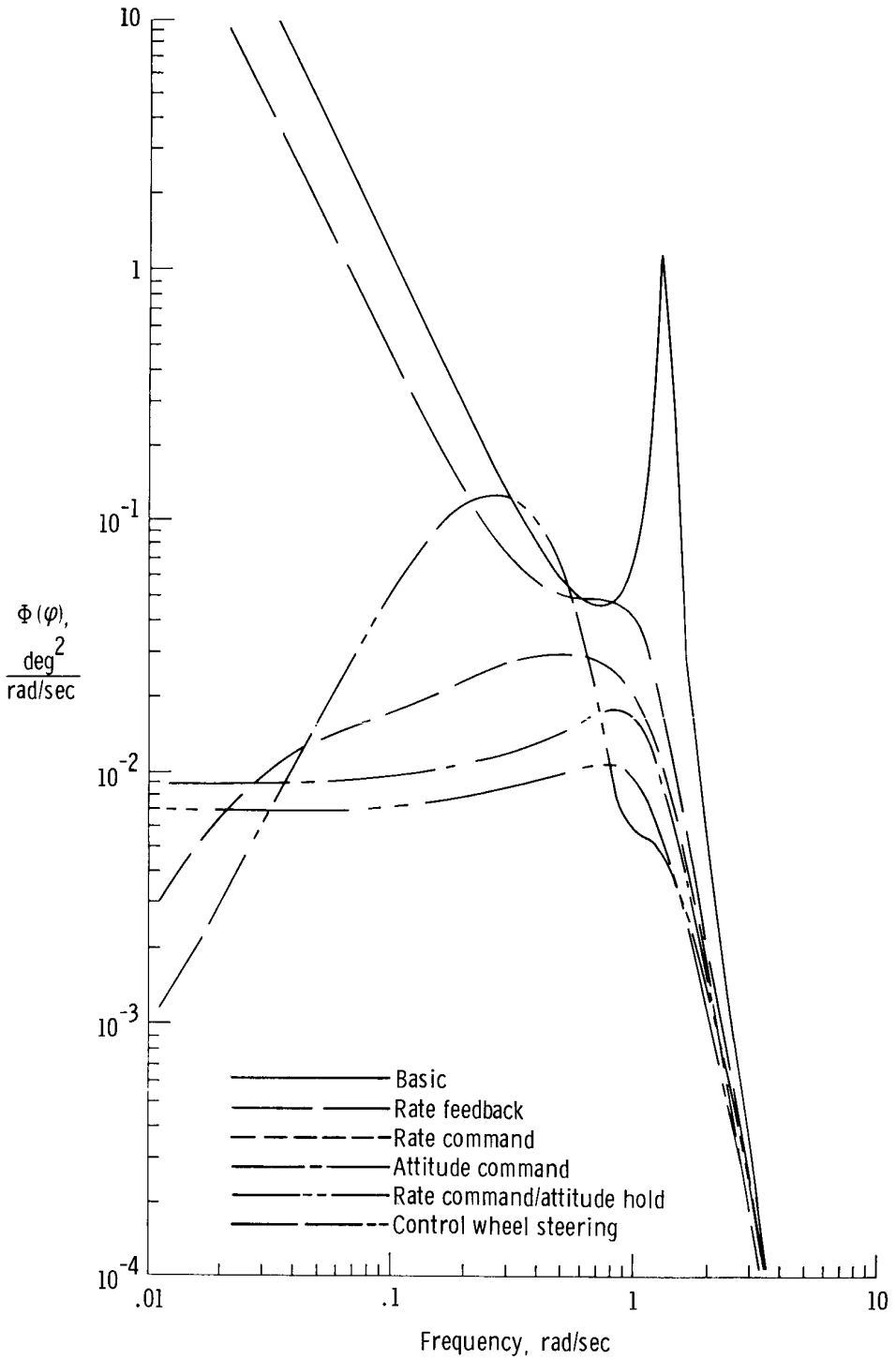

(e) Bank angle.

Figure 14. Continued.

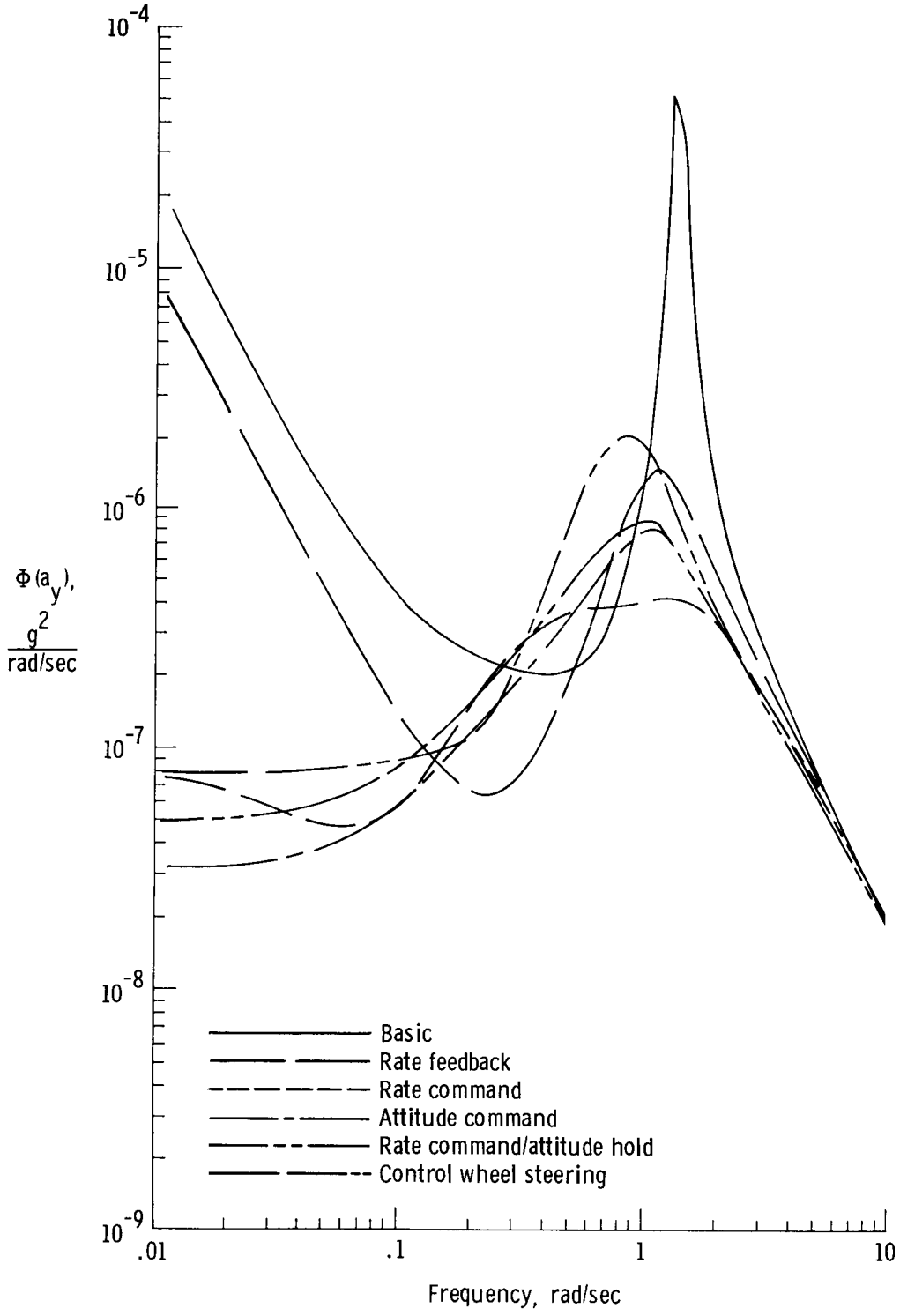

(f) Lateral acceleration.

Figure 14. Concluded.

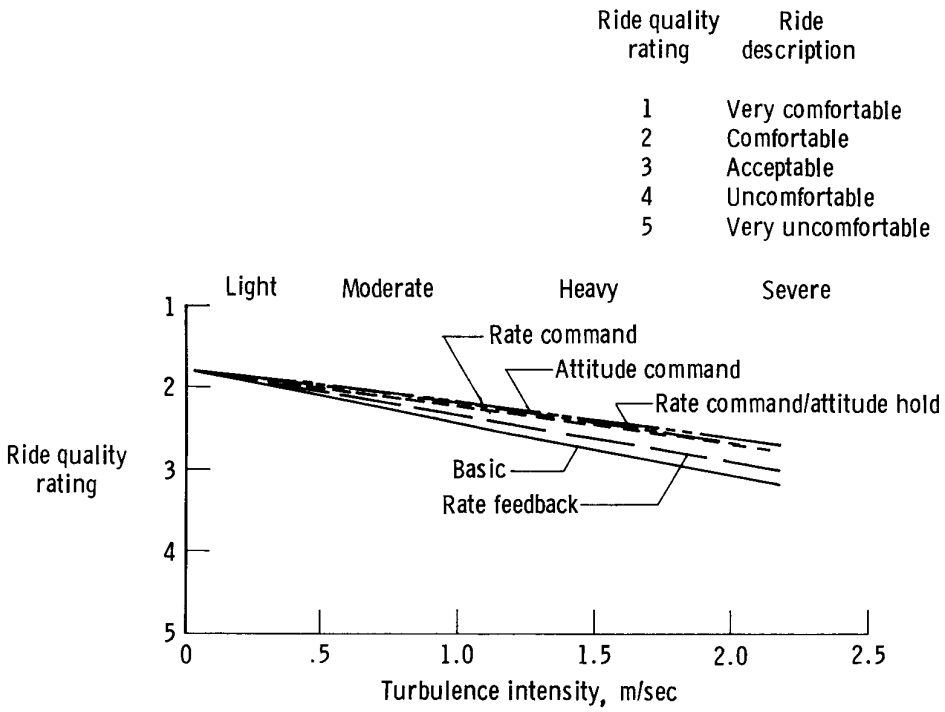

(a) Reference 7 model.

Figure 15. Calculated ride quality ratings using the ride quality models of references 7 to 9.

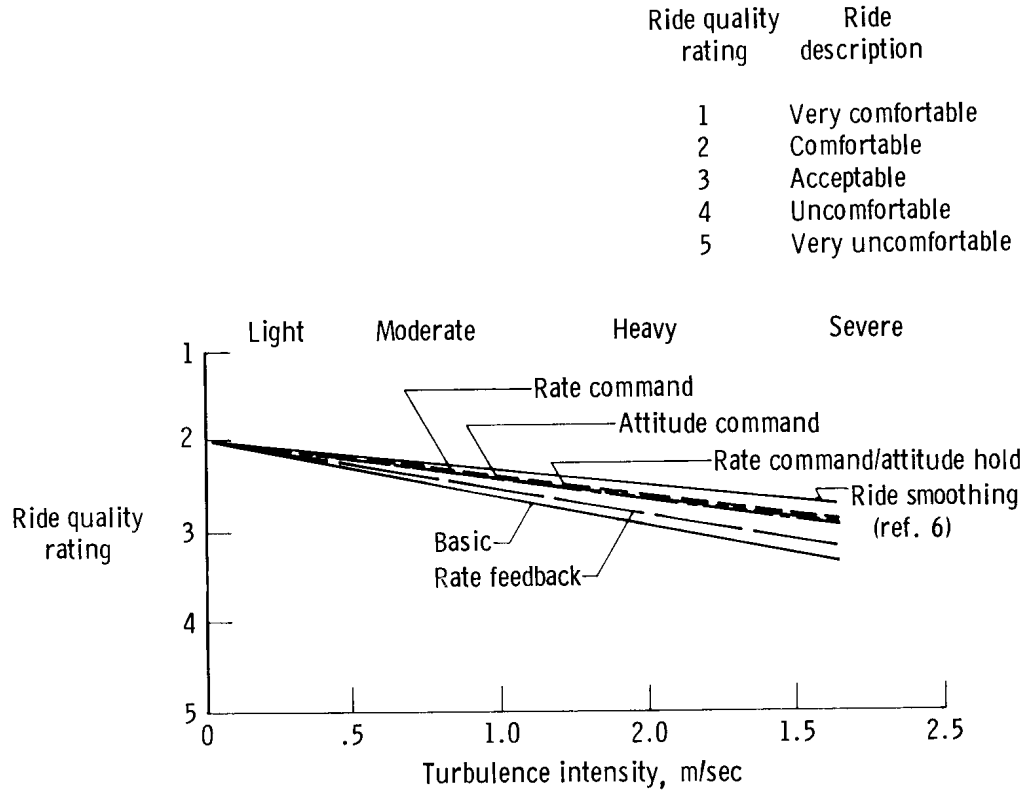

(b) Reference 8 model.

Figure 15. Continued.

Ride quality rating	Ride description
1	Very comfortable
2	Comfortable
3	Acceptable
4	Uncomfortable
5	Very uncomfortable

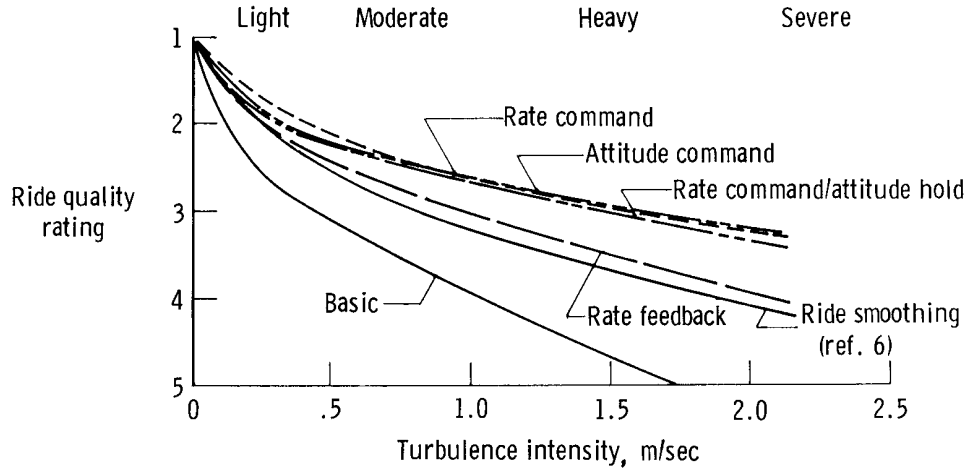

(c) Reference 9 model.

Figure 15. Concluded.

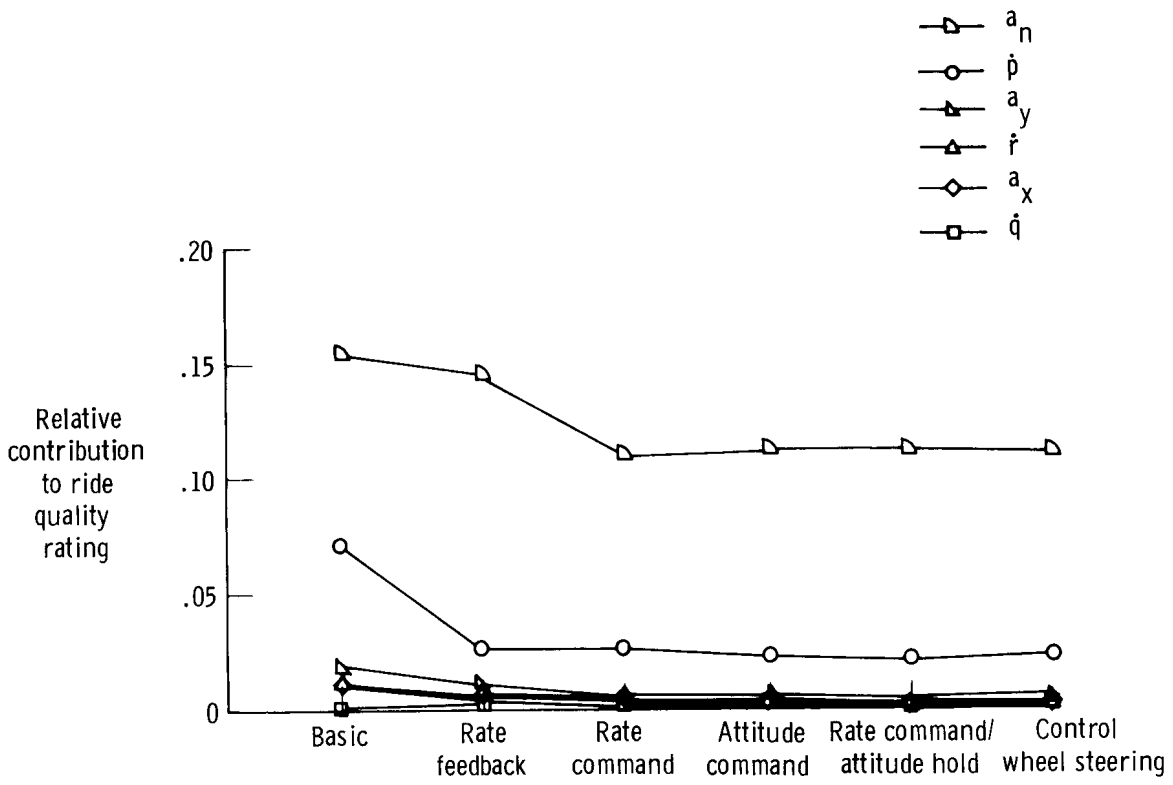

(a) Reference 7 model, 0.3-meter-per-second rms turbulence input.

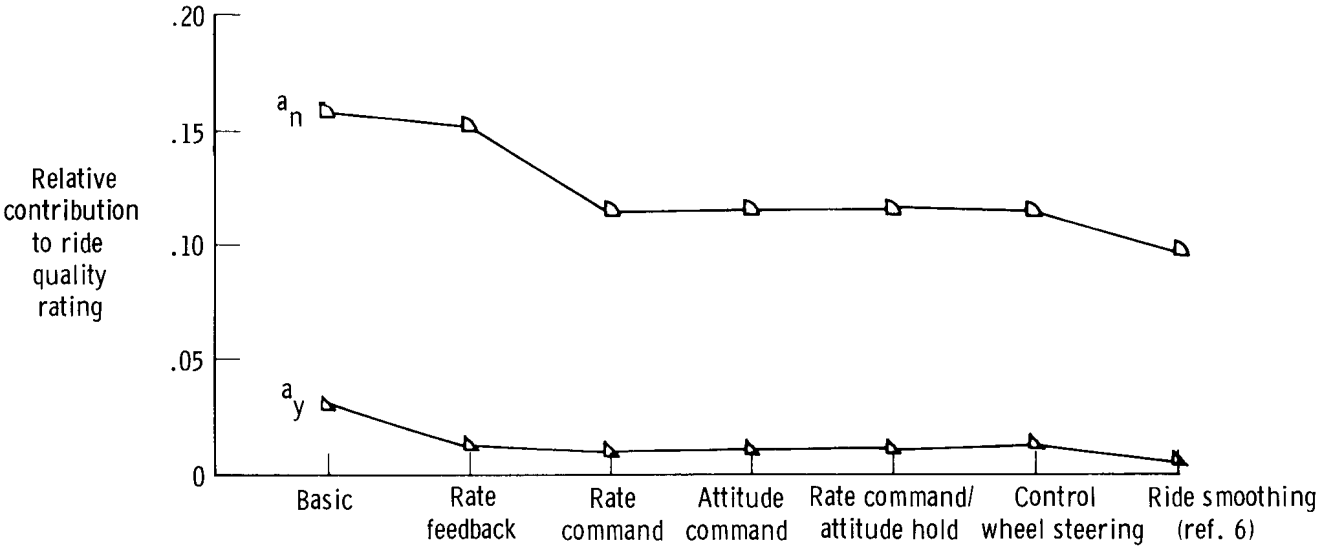

(b) Reference 8 model, 0.3-meter-per-second rms turbulence input.

Figure 16. Effect of various types of motion on ride quality ratings using ride quality models in references 7 to 9.

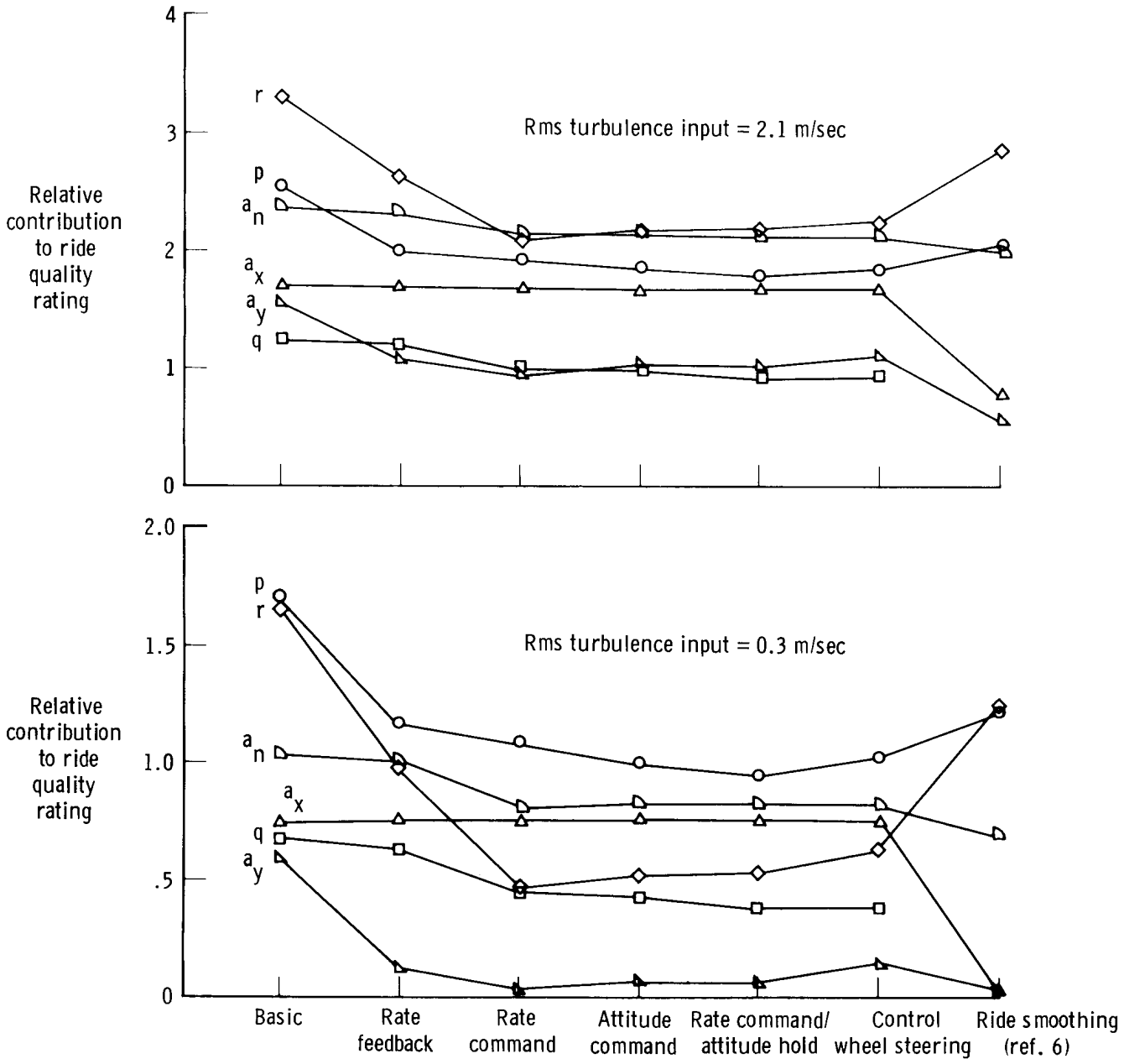

(c) Reference 9 model for two turbulence levels.

Figure 16. Concluded.

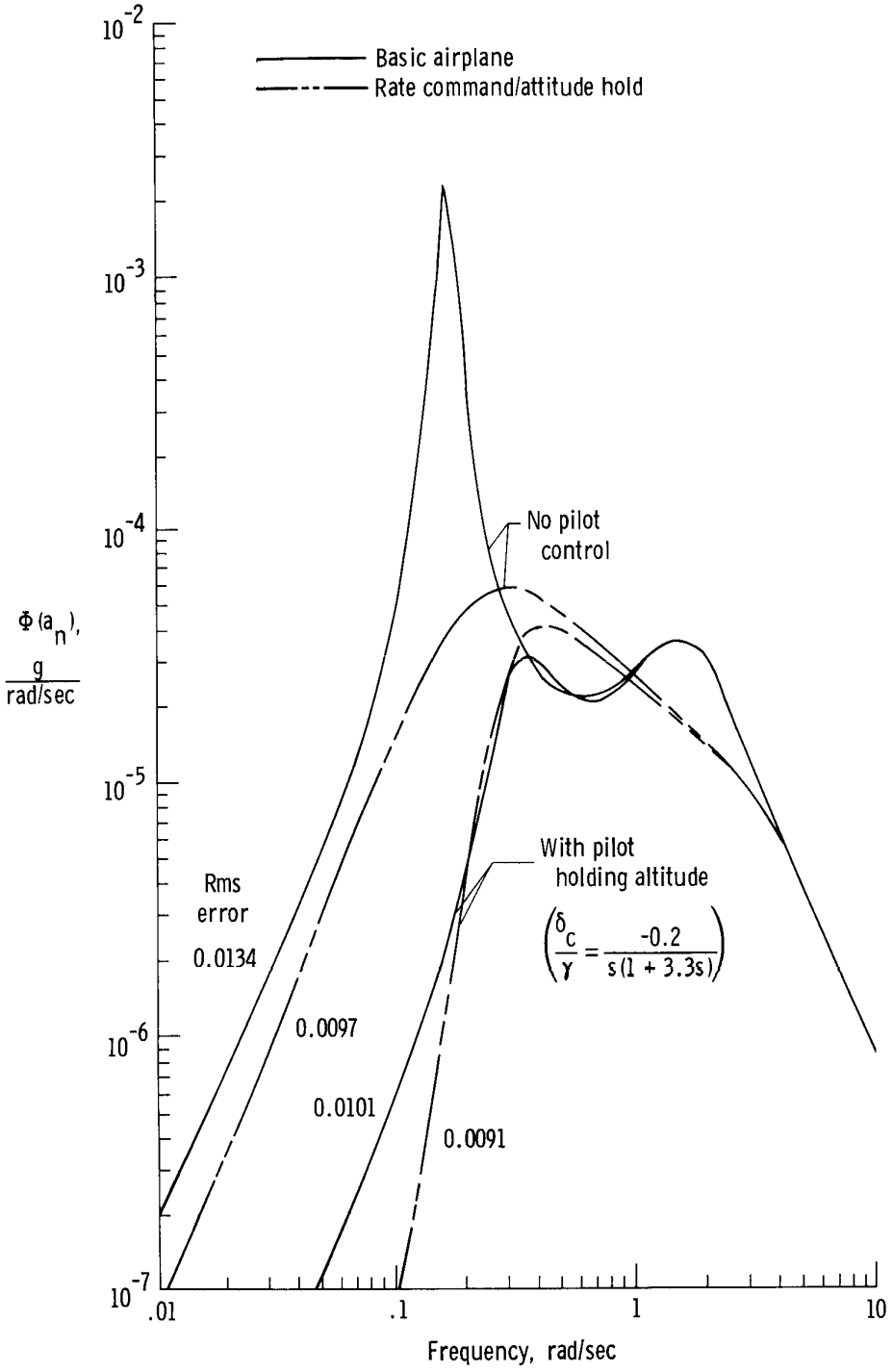

Figure 17. Effect of pilot altitude feedback on a_n power spectral density.

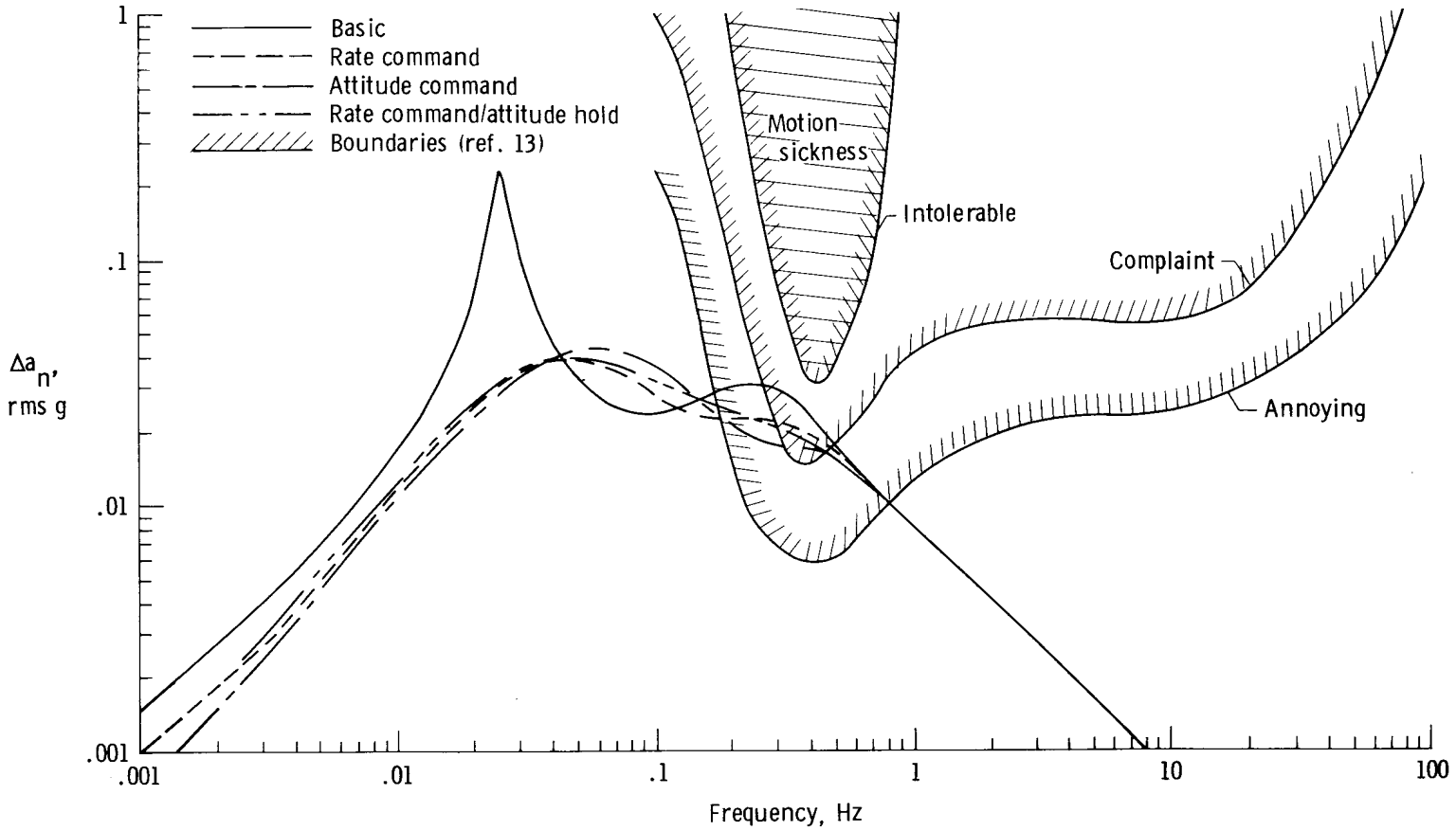

Figure 18. Normal acceleration responses for a 1.5-meter-per-second rms turbulence input (heavy turbulence) and the criteria from reference 13.

1. Report No.	2. Government Accession No.	3. Recipient's Catalog No.
NASA TP-1148		

4. Title and Subtitle	5. Report Date
ANALYTICAL STUDY OF RIDE SMOOTHING BENEFITS OF CONTROL SYSTEM CONFIGURATIONS OPTIMIZED FOR PILOT HANDLING QUALITIES	February 1978
	6. Performing Organization Code: H-922
7. Author(s): Bruce G. Powers	8. Performing Organization Report No.
	10. Work Unit No.: 505-06-91
9. Performing Organization Name and Address: NASA Dryden Flight Research Center, P.O. Box 273, Edwards, California 93523	11. Contract or Grant No.
	13. Type of Report and Period Covered: Technical Paper
12. Sponsoring Agency Name and Address: National Aeronautics and Space Administration, Washington, D.C. 20546	14. Sponsoring Agency Code

15. Supplementary Notes

16. Abstract

An analytical study was conducted to evaluate the relative improvements in aircraft ride qualities that resulted from utilizing several control law configurations that were optimized for pilot handling qualities only. The airplane configuration used was an executive jet transport in the approach configuration. The control law configurations included the basic system, a rate feedback system, three command augmentation systems (rate command, attitude command, and rate command/attitude hold), and a control wheel steering system. Both the longitudinal and lateral-directional axes were evaluated. A representative example of each control law configuration was optimized for pilot handling qualities on a fixed-base simulator. The root mean square airplane responses to turbulence were calculated, and predictions of ride quality ratings were computed by using three models available in the literature.

17. Key Words (Suggested by Author(s))	18. Distribution Statement
Ride smoothing Handling qualities Control systems	Unclassified—Unlimited STAR Category: 08

19. Security Classif. (of this report)	20. Security Classif. (of this page)	21. No. of Pages	22. Price*
Unclassified	Unclassified	61	$4.25

For sale by the National Technical Information Service, Springfield, Virginia 22161

NASA-Langley, 1977